

ARTICLE

Methods, Tools, and Technologies

Young forests and fire: Using lidar–imagery fusion to explore fuels and burn severity in a subalpine forest reburn

Kristin H. Braziunas¹  | Diane C. Abendroth² | Monica G. Turner¹ 

¹Department of Integrative Biology,
 University of Wisconsin-Madison,
 Madison, Wisconsin, USA

²Teton Interagency Fire, Grand Teton
 National Park, Moose, Wyoming, USA

Correspondence

Kristin H. Braziunas
 Email: kristin.braziunas@tum.de

Present address

Kristin H. Braziunas, TUM School of Life Sciences, Technical University of Munich, 85354 Freising, Germany

Funding information

National Park Service Fuels Reserve Fund, Grant/Award Number: P17AC01466; P.E. O. Ventura Neale Trust Endowed Scholar Award; University of Wisconsin Vilas Trust

Handling Editor: Debra P. C. Peters

Abstract

Anticipating fire behavior as climate change and fire activity accelerate is an increasingly pressing management challenge in fire-prone landscapes. In subalpine forests adapted to infrequent, stand-replacing fire, self-limitation of burn severity in short-interval fire is incompletely understood. Spatially explicit fuels data can support assessments of landscape-scale fire risk and fuel feedbacks on burn severity. For a ~1450-km² largely forested landscape in the US Northern Rocky Mountains, we used airborne lidar and imagery to predict and map canopy and surface fuels. In a fire that burned mature (>125-year-old) and also reburned young (~30-year-old) subalpine forest, we then asked: (1) How do prefire fuels and burn severity compare between young and mature forests that burned under similar fire weather conditions? (2) How well do prefire fuels and forest structure predict burn severity under extreme versus moderate fire weather? Lidar–imagery fusion predicted fuel characteristics with high accuracy across forest and shrubland vegetation. Young postfire forests had abundant, densely packed canopy fuels, and both young and mature forests had similar canopy fuel loads and coarse wood biomass. Under similar weather conditions, young and mature forests burned at similar severity. Overall, fuels were weak predictors of burn severity and, surprisingly, better predicted severity under extreme rather than moderate fire weather. Our findings are relevant for subalpine landscapes increasingly dominated by young lodgepole pine (*Pinus contorta* var. *latifolia*) forests vulnerable to short-interval fire and provide a benchmark to assess how fuels influence burn severity in future fires. Fire managers should continually reassess fuels and update expectations about fire behavior as landscapes change. Although recovering postfire forests can limit fire spread and severity for a period of time, our results suggest that young subalpine forests in the Northern Rocky Mountains have sufficient fuel loads to burn at high severity and should not be considered effective fire breaks.

KEY WORDS

canopy and surface fuels, fire effects, Grand Teton National Park, lidar–imagery fusion, Northern Rocky Mountains, short-interval fire

This is an open access article under the terms of the [Creative Commons Attribution License](#), which permits use, distribution and reproduction in any medium, provided the original work is properly cited.

© 2022 The Authors. *Ecosphere* published by Wiley Periodicals LLC on behalf of The Ecological Society of America.

INTRODUCTION

The rapid rise in fire activity across the western United States (Higuera & Abatzoglou, 2021; Westerling, 2016) is challenging the ability of land managers to anticipate fire behavior and effectively allocate limited resources for fire suppression or fuels treatment (BAH, 2015; WFEC, 2014). When possible, fire managers also identify opportunities for allowing fires or portions of fires to burn or for using prescribed fire to achieve resource benefits such as restoring historical vegetation structures and reducing fuel loads (Meyer et al., 2015; WFEC, 2014). These choices must be made in an increasingly difficult decision-making environment characterized by lengthening fire seasons (Westerling, 2016), more extreme fire weather (Abatzoglou & Williams, 2016), larger and more severe fires (Cansler & McKenzie, 2014), expanding wildland urban interface communities (Radeloff et al., 2018), widespread human ignitions (Balch et al., 2017), and legacies of fire exclusion leading to fuel accumulation in some forest types (Stephens et al., 2013). US governmental agencies use spatial assessments of fire progression and risk to manage long-duration fires (Calkin et al., 2011; O'Connor et al., 2016). Fire risk assessments depend on two critical inputs that require additional refinement: spatially explicit fuels data and an understanding of how fuels influence burn severity under varying weather conditions.

Vegetation structure and fuels vary substantially across heterogeneous landscapes (Keane et al., 2012), but most landscapes lack accurate canopy and surface fuels maps. The LANDFIRE program enhanced fire risk planning capabilities by providing national, wall-to-wall fuels maps for fire behavior models (Ryan & Opperman, 2013). However, LANDFIRE's utility is limited for fine-scale applications. Canopy fuels are predicted with low accuracy in many vegetation types (Keane et al., 2006; Moran et al., 2020; Reeves et al., 2009), and fuels data must be quality checked and calibrated prior to use (Stratton, 2009). Locally derived maps can improve predictions of fuel characteristics (Engelstad et al., 2019) and fire spread (Krasnow et al., 2009). In addition, surface fuels are mapped as categorical fuel models or fuel beds that are primarily suited for estimating fire behavior and effects and may not accurately predict actual fuel loads (Hyde et al., 2015; Keane et al., 2013). Incorporating local data to improve vegetation structure and surface fuels maps could support better estimation of wildlife habitat (Harmon et al., 1986); carbon storage, fire combustion, and smoke emissions (Weise & Wright, 2014); and optimal firefighter escape routes (Campbell et al., 2017) and safety zones (Dennison et al., 2014).

Anticipating fire behavior as climate change and fire activity accelerate is an increasingly pressing challenge in

fire-prone landscapes where vegetation may reburn more frequently than their historical baseline (Coop et al., 2020; Enright et al., 2015; Halofsky et al., 2020; Prichard et al., 2017). In many forests throughout western North America, burned areas can limit subsequent fire spread and severity due to reduced postfire fuel loads and continuity, but the duration of self-limitation varies by forest type, burn severity, fire season weather, and trajectories of postfire fuels development (McKenzie et al., 2011; Parks et al., 2014, 2015; Stevens-Rumann et al., 2016; see tab. 2 in Prichard et al., 2017). In US Northern Rocky Mountain subalpine forests where lodgepole pine (*Pinus contorta* var. *latifolia*) dominates postfire succession, self-regulation was previously thought to last >100 years for spread and even longer for severity due to slow development of fuels capable of supporting crown fire (Despain & Sellers, 1977; Romme, 1982). This assumption did not hold when fires in 1988 severely burned extensive areas of forests of all ages under extremely dry and windy conditions (Renkin & Despain, 1992; Romme & Despain, 1989). Recent studies suggest that initial burning may only limit subsequent fire spread for ~10–20 years in western US forests (Buma et al., 2020; Prichard et al., 2017), but effects on subsequent burn severity are less clear. Some studies conclude that areas of high-severity fire are more likely to reburn severely after only 10–12 years (Harvey et al., 2016), whereas others indicate that burn severity is self-regulated for decades (Parks et al., 2014; Stevens-Rumann et al., 2016) or more than a century (Bigler et al., 2005). In less than 25 years, lodgepole pine forests regenerating from stand-replacing fire can accumulate sufficient canopy and surface fuels to support crown fire (Nelson et al., 2016, 2017) and to reburn as stand-replacing fire (Turner et al., 2019). However, whether fuel loads and continuity in young subalpine forests support high-severity fire across extensive reburned areas and how strongly fuels limit burn severity in reburns are incompletely understood.

Spatial data on vegetation structure and fuels can be used to quantify relationships between fuels and burn severity in reburns. Fuels, weather, and topography interact to influence burn severity, and fuels tend to be a limiting factor in dry forests adapted to frequent, low-severity fire (Schoennagel et al., 2004). In moist subalpine forests that typically burn infrequently and at high severity, fuels are usually plentiful and extreme fire weather is the dominant driver of fire behavior (Bessie & Johnson, 1995; Turner et al., 1994; Turner & Romme, 1994). However, these relationships may shift if subalpine forests change from climate- to fuel-limited systems under increasingly frequent fire (Hessburg et al., 2019). Studies exploring the relationship between fuels and burn severity (e.g., Bessie & Johnson, 1995; Nelson et al., 2017; Parks et al., 2018; Stevens-Rumann et al., 2016) often rely on fuels data from sparse field plots, simulated fire behavior, or national maps.

A spatially continuous, accurate fuels map overcomes many of the limitations of other approaches, which include high sampling effort or sampling bias (field plots), deterministic relationships between fuels and severity (simulated fire behavior), and low accuracy of predicted fuels (national maps). In this study, we combined airborne light detection and ranging (lidar), aerial imagery, and field data to map fuels in forests and

shrublands across a large landscape centered on Grand Teton National Park (Wyoming, USA; Figure 1). Airborne lidar and imagery fusion can characterize three-dimensional vegetation structure and fuels at landscape scales with high spatial resolution (Lefsky et al., 2002; Lepczyk et al., 2021; Szpakowski & Jensen, 2019). We expected lidar–imagery fusion would best predict fuel metrics nearest to the top of the canopy (e.g., canopy

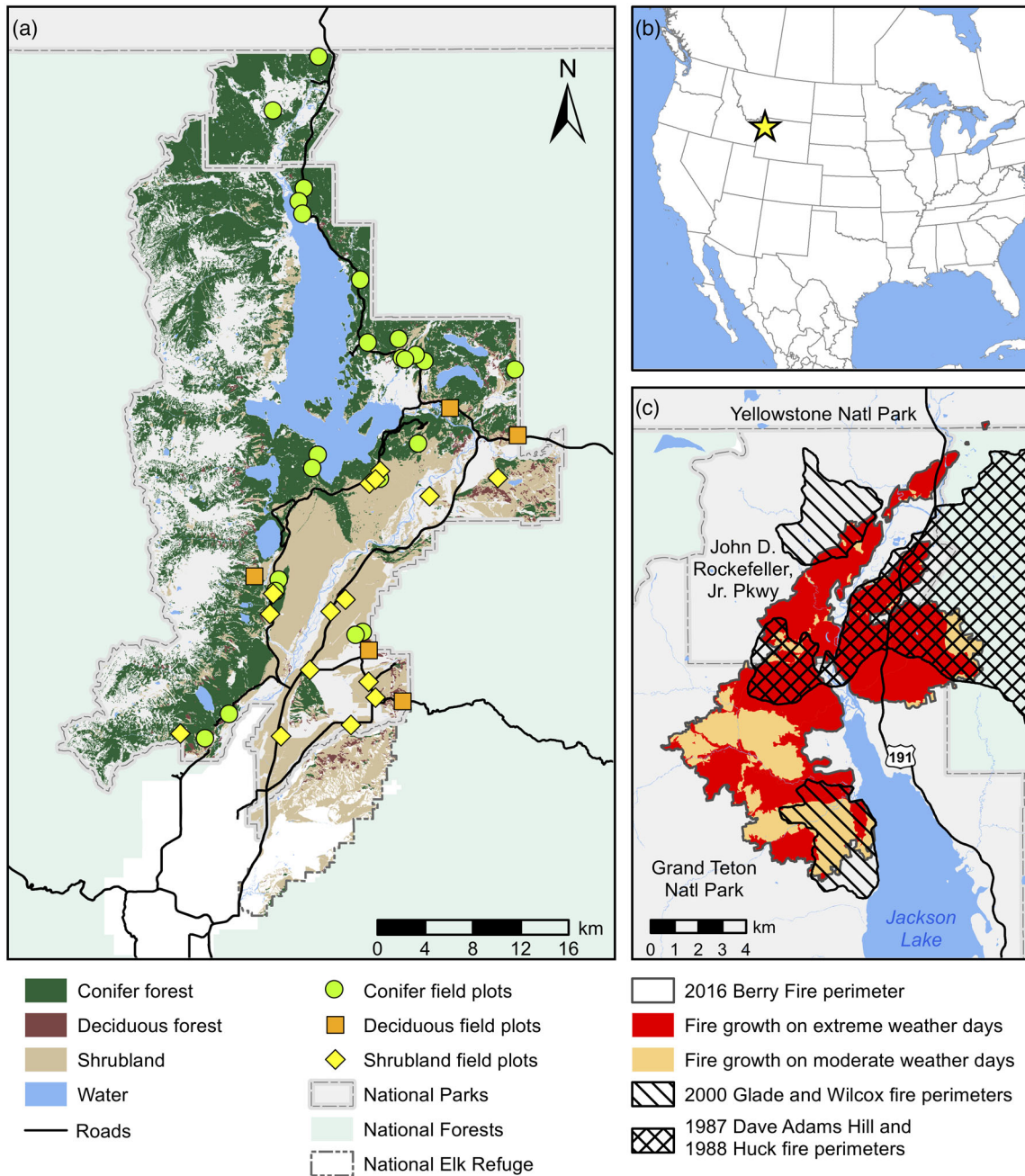


FIGURE 1 (a) Vegetation map and 2019 field plot locations within the footprint of the final fuels map, including Grand Teton National Park, John D. Rockefeller, Jr. Memorial Parkway, and the National Elk Refuge. (b) Location of study area (star) within North America. (c) 2016 Berry Fire footprint. Colors show areas within the footprint that burned under extreme (red) and moderate (orange) fire weather. Lines identify areas that reburned 1987 or 1988 fire perimeters (crosshatched) or 2000 fire perimeters (parallel lines).

height and cover) and decrease in goodness-of-fit for within-canopy fuels (e.g., canopy base height; Andersen et al., 2005; Chamberlain et al., 2021; Erdody & Moskal, 2010; Jakubowski et al., 2013). In forests, we expected lowest predictive power for surface fuels, which included downed coarse woody debris (CWD) and shrubs, although CWD has been successfully derived from lidar in some forest types (Blanchard et al., 2011; Joyce et al., 2019; Pesonen et al., 2008; Tanhuanpää et al., 2015; van Aardt et al., 2011). We did not expect lidar to effectively differentiate between finer surface fuels (e.g., litter, duff, fine wood, and herbaceous fuels) under forest canopies, so these were not mapped.

We then used this map to ask two questions in a subalpine forest reburn: (1) How do prefire fuels and burn severity compare between young (~30-year-old) and mature (>125-year-old) forests that burned under similar fire weather conditions? We expected young forests to have similar or higher fuel loads and burn severity, as well as lower canopy base heights, relative to mature forests (Nelson et al., 2016; Turner et al., 2019). (2) How well do prefire fuels and forest structure predict burn severity under extreme versus moderate fire weather? We expected fuels and forest structure to be weak predictors of burn severity despite the presence of large areas of young forest within the fire perimeter, because young forests would not be fuel limited. However, we expected fuels would better predict burn severity under moderate versus extreme fire weather, because under extreme conditions the influence of weather would overwhelm that of fuels (Bessie & Johnson, 1995; Collins et al., 2019; Meigs et al., 2020).

METHODS

Study area

The study area encompasses ~1450 km² in northwest Wyoming in the US Northern Rocky Mountains and includes Grand Teton National Park, the John D. Rockefeller, Jr. Memorial Parkway, and the National Elk Refuge (hereafter collectively referred to as “GRTE”; Figure 1). Along with Yellowstone National Park and several national forests, GRTE anchors the Greater Yellowstone Ecosystem, a 89,000-km² area that is one of the largest protected temperate ecosystems on Earth (YNP, 2017). The GRTE is bounded on the west by the Teton Range, and elevations span 1900 m along the Jackson Hole Valley to 4200 m at the summit of Grand Teton (Cogan et al., 2005). Shrublands dominated by mountain big sagebrush (*Artemesia tridentata* ssp. *vaseyanus*) characterize the lower-elevation, relatively flat valley floor

(Figure 1a). Montane and subalpine conifer forests cover most of the vegetated area of the park. Dominant forest types include low- to mid-elevation lodgepole pine forests and Douglas-fir (*Pseudotsuga menziesii* var. *glauca*) woodlands, higher-elevation subalpine fir (*Abies lasiocarpa*)–Engelmann spruce (*Picea engelmannii*) forests, and whitebark pine (*Pinus albicaulis*) forests near upper treeline (3000 m). Small pockets of deciduous forests dominated by quaking aspen (*Populus tremuloides*) are interspersed at intermediate elevations. Given complex and variable topographic conditions and disturbance histories throughout the landscape, forest types and tree species are often intermixed. At lower elevations, summers are warm and dry with a mean July temperature of 16.6°C and 554 mm of annual precipitation, most of which falls as snow (Moose, Wyoming, 1981–2010 climate normals; WRCC, 2020a). Temperatures cool and precipitation increases at higher elevations.

Throughout the US Northern Rocky Mountains, conifer forests and woodlands have historically burned infrequently at high or mixed severity, though lower-elevation forest types also burn at low severity at shorter fire intervals (Baker, 2009). For over 10,000 years, Indigenous peoples including the Eastern Shoshone, Shoshone-Bannock, Blackfeet, Crow (Apsáalooke), Salish Kootenai (Flathead), Aaniiih (Gros Ventre), and Niimiipu (Nez Perce) peoples occupied and used land in Greater Yellowstone before being forcibly removed during the creation of the National Parks (Native Land Digital, 2021; Spence, 1999). Indigenous burning is well documented throughout the western United States, but evidence suggests that climate remained the dominant driver of fire regimes in higher-elevation forests of the Northern Rocky Mountains except in localized areas such as settlements and travel routes (Baker, 2002; Whitlock et al., 2010). In subalpine, lodgepole pine-dominated forests, stand-replacing fires typically occurred every 100–300 years during periods of extreme drought and high winds (Bessie & Johnson, 1995; Higuera et al., 2011; Renkin & Despain, 1992; Romme & Despain, 1989; Whitlock et al., 2008). In Grand Teton National Park and the Jackson Hole Valley, extensive, stand-replacing fires occurred in the late 1800s, initiating synchronous, widespread postfire regeneration of lodgepole pine and aspen (Brandegee, 1898; Loope & Gruell, 1973). Many of the older mixed conifer, Douglas-fir, and spruce-fir stands originated from stand-replacing fire in the 1600s–1700s (Sibold et al., 2014). Fires were suppressed during a portion of the 20th century, but past fire suppression was not always effective and had minimal effects on the stand-replacing fire regimes that characterize forest types in this region (Hansen et al., 2020; Schoennagel et al., 2004; Turner et al., 1994). Except for a few years following the 1988 fire season, wildfires have been allowed to burn for resource

benefits since 1972 in GRTE when they are not a threat to life or infrastructure (GRTE, 2009; Knight et al., 2014; Loope & Wood, 1976). Annual area burned over the past 50 years has been relatively low compared to the full extent of the study area, but there have been 11 years with >1000 ha burned, most of which have occurred since the year 2000.

The 2016 Berry Fire

The largest fire in recorded GRTE history, the Berry Fire was discovered on 25 July 2016 and burned 8143 ha over more than 2 months, mostly in subalpine, lodgepole pine-dominated forest (Figure 1c; MTBS Project, 2019). The lightning-ignited fire burned entirely within national park or national forest areas and was managed primarily for ecological objectives. The Berry Fire included 4 days (22 August, 23–24 August, and 11 September) of high fire spread under extreme fire weather characterized by dry conditions and high wind (6077 ha burned, 28% average relative humidity with maximum wind gusts between 43 and 82 km h^{-1} ; GeoMAC, 2016; WRCC, 2020b). The remaining 2066 ha burned under more moderate fire weather (44% average relative humidity with maximum

wind gusts between 23 and 61 km h^{-1}). In addition to burning mature (>125 -year-old; Brandegee, 1898; Sibold et al., 2014) forest, 43% of the Berry Fire reburned <30 -year-old forest regenerating following the 1987 Dave Adams Hill Fire, 1988 Huck Fire, 2000 Glade Fire, and 2000 Wilcox Fire.

Predicting and mapping forest and shrubland structure and fuels

We adapted established best practices to map vegetation attributes from airborne lidar and imagery (Figure 2; Laes et al., 2011; Mitchell et al., 2012; White et al., 2013).

Data sources and initial processing

Airborne discrete-return, medium-resolution (0.7 m nominal pulse spacing and up to 4 returns pulse $^{-1}$, resulting in 5.7 points m^{-2}), lidar data were collected using a Leica ALS70 sensor for GRTE during summer 2014 (Woolpert, 2015). Woolpert (2015) reviewed, classified, and processed lidar point clouds; vertical accuracy of bare earth points was 0.074 m root-mean-squared error

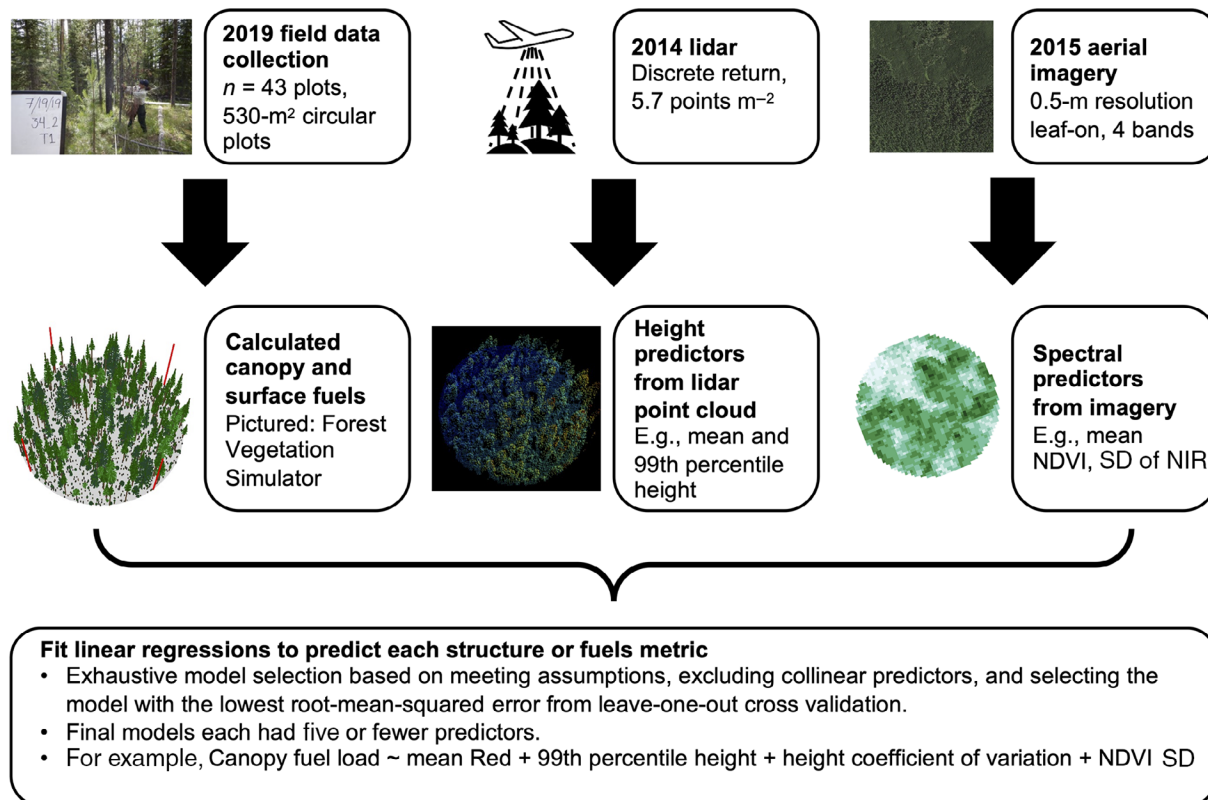


FIGURE 2 Flow chart outlining methods for using lidar-imagery fusion with field data collection to map canopy and surface fuel characteristics. NDVI, normalized difference vegetation index; NIR, near infrared; SD, standard deviation

(RMSE). We prepared point clouds for plot selection and analysis by removing points classified as noise, buildings, water, ignored ground, and overlap and reclassifying remaining nonground points as surface (0.1- to 2-m height) or canopy vegetation (2–60 m). Points >60-m height were excluded from further analysis based on the maximum height of dominant conifers (Braziunas et al., 2018; Burns & Honkala, 1990).

We acquired 2015 leaf-on aerial imagery for visible and near-infrared bands (0.5-m resolution) from the National Agriculture Imagery Program (NAIP; NAIP, 2015). We also obtained a 2005 vegetation map for the study region, which had an overall thematic accuracy of 82% (Cogan et al., 2005). We used three broad vegetation types to guide our study design and analysis: conifer forest, deciduous forest, and shrubland (Figure 1a).

Field data collection

Vegetation structure and fuels were sampled during summer 2019. We first excluded areas that were disturbed or managed after acquisition of remotely sensed data (GRTE, unpublished data; USDA Forest Service, 2019). We then used stratified random sampling to select plots based on vegetation type, lidar-derived 90th percentile canopy height, and lidar-derived canopy (forests) or shrub (shrublands) cover (see Appendix S1: Table S1). We additionally sampled two plots that represented target conditions: first, dense young forest regenerating from severe fire, and second, sparse postfire recovery with abundant downed wood. All plots were separated by >500 m except for two that were 290 m apart. In total, we sampled 43 circular 530-m² plots (23 conifer, 15 shrubland, and 5 deciduous; plot radius = 13 m) that covered a wide range of site, vegetation structure, and fuels conditions (Table 1, Figure 1a). We recorded plot center with a Trimble Geo 7X. Average postprocessed horizontal precision was 0.12 m, and average vertical precision was 0.16 m.

To quantify forest structure and canopy fuels in field plots, we measured the dbh, species, and status (live, dead, or dead with foliage) of every tree >1.4 m in height. Trees at plot edges were counted if >50% of their crown was within the plot. For all trees >7.6 cm dbh, we also recorded tree height and crown base height. We developed species-specific regression models to estimate height and crown base height of smaller trees <7.6 cm dbh. Due to the time lag between the lidar flight and field data collection, we assumed dead trees with foliage in 2019 were alive in 2015 and included them in structure and fuel metric calculations. For one plot in which tree density exceeded 35,000 stems ha⁻¹, individual trees were counted in only one-fourth of the plot area. Live saplings

between 0.1 and 1.4 m in height were tallied by species in a 2 × 26-m belt transect (total area = 52 m²). Average sapling height was estimated by measuring the height of one stem closest to each 5-m mark along the transect.

To quantify surface fuel characteristics, we established two perpendicular transects that intersected at plot center, with a 1-m buffer to avoid double-counting (total length = 50 m). We used Brown's planar intercepts (Brown, 1974) to measure CWD (1000-h fuels, >7.6 cm diameter) and line intercepts (Couloudon et al., 1999) to measure sapling/shrub cover and height by species. We included trees <2-m height in shrub line intercepts because the surface fuel layer includes all vegetation up to 2 m in height (Keane, 2015). We estimated sapling/shrub percent dead in eight 0.5-m² quadrats spaced a minimum of 5 m apart along each transect (total area = 2 m²).

Derivation of fuel and structure metrics from field data

Forest structure, CWD cover and biomass, and sapling/shrub cover and height were derived following standard methods (Table 1, Figure 2; Brown, 1974; Couloudon et al., 1999). We used Forest Vegetation Simulator (FVS; Dixon, 2002) Complete Package Software Version 2020.03.11 to quantify canopy fuel metrics, including canopy height and cover, based on the Tetons Variant (Keyser & Dixon, 2008). The FVS uses species-specific allometric equations for a given variant to estimate fuel loads within the canopy. Canopy fuels are defined and calculated in different ways. Following FVS, we defined canopy fuel load as standing live foliage biomass, canopy bulk density (CBD) as the maximum 13-ft (4-m) running mean within the canopy fuel profile, and canopy base height (CBH) as the lowest height at which CBD exceeds 0.011 kg m⁻³ (Rebain, 2010; Scott & Reinhardt, 2001).

Derivation of potential predictor variables from lidar and imagery

We clipped lidar and imagery to plot boundaries and derived a suite of potential predictor values based on their success in predicting fuels in previous studies (Appendix S1: Table S1; Figure 2; Erdody & Moskal, 2010). Lidar predictors included summary vegetation height statistics, canopy cover, and shrub cover. From NAIP imagery, we calculated 0.5-m resolution pseudo-normalized difference vegetation index (NDVI) from the red and near-infrared bands (Jensen, 2007) and texture homogeneity for all bands within a 7 × 7 moving window (Moskal & Franklin, 2002). Imagery predictors included summary statistics

TABLE 1 Topographic conditions, forest structure, and fuel metrics for plots sampled in 2019

| Measurement | Description | Conifer forest (n = 23) | Deciduous forest (n = 5) | Shrubland (n = 15) |
|--|---|------------------------------|-----------------------------|------------------------|
| Topographic conditions | | | | |
| Elevation (m) | Elevation at plot center | 2091 (55) 1944–2217 | 2083 (30) 2052–2128 | 2045 (50) 1959–2155 |
| Slope (°) | Dominant slope | 5 (5) 0–16 | 9 (5) 3–14 | 4 (7) 0–26 |
| Aspect (°) | Dominant aspect (excludes two plots that were flat) | 200 (107) 6–356 | 170 (98) 92–302 | 215 (84) 76–314 |
| Forest structure | | | | |
| Tree density (stems ha ⁻¹) | Density of trees >1.4 m height | 3573 (7269) 170–36,238 | 2972 (1694) 1149–5575 | — |
| Tree basal area (m ² ha ⁻¹) | Basal area for trees >1.4 m height | 23.1 (10.5) 0.8–37.5 | 21.6 (16.5) 8.1–47.5 | — |
| Sapling density (stems ha ⁻¹) | Density of saplings between 0.1 and 1.4 m height | 7926 (19,059) 0–93,846 | 3192 (2899) 0–7308 | — |
| Sapling height (m) | Mean height of saplings between 0.1 and 1.4 m height. Excludes plots where no saplings present | 0.7 (0.2) 0.4–1.0 | 0.9 (0.0) 0.9–1.0 | — |
| Canopy fuel layer | | | | |
| Canopy cover (CC, %) | Vertically projected cover of the suspended canopy onto the ground | 41 (15) 5–63 | 66 (22) 40–93 | — |
| Canopy height (CH, m) | Average height of the top of the vegetated canopy | 18.5 (7.2) 4.3–34.1 | 12.9 (6.2) 9.1–23.8 | — |
| Canopy fuel load (CFL, kg m ⁻²) | Amount of canopy fuel consumed in a crown fire. Quantified as standing live foliage biomass | 1.00 (0.45) 0.03–1.85 | — | — |
| Canopy bulk density (CBD, kg m ⁻³) | Amount of burnable canopy biomass in a given volume of space. Quantified as maximum 13-ft (4-m) running mean within the canopy fuel profile (Rebain, 2010; Scott & Reinhardt, 2001) | 0.093 (0.045) 0.009–0.194 | — | — |
| Canopy base height (CBH, m) | Lowest height at which CBD exceeds 0.011 kg m ⁻¹ (Rebain, 2010; Scott & Reinhardt, 2001) | 0.6 (0.5) 0.3–2.4 | — | — |
| Surface fuel layer | | | | |
| Coarse woody debris (CWD) cover (%) | Cover of downed coarse woody debris (1000-h woody fuels, >7.6 cm diameter) | 11 (7) 3–24 | 4 (3) 0–10 | — |
| CWD biomass (Mg ha ⁻¹) | Quantified following Brown (1974), includes sound and rotten, adjusted for slope | 62.4 (39.8) 7.7–151.2 | 20.6 (20.4) 0–54.8 | — |
| Sapling/shrub cover (%) | Percent cover of surface fuel layer, which includes all shrubs >0.1-m height and trees <2-m height | 22 (14) 5–51 | 24 (15) 3–46 | 42 (17) 16–77 |
| Sapling/shrub height (m) | Average height of surface fuel layer. Average height is based on top height of individual shrubs and weighted by species percent cover | 0.7 (0.3) 0.3–1.4 | 0.7 (0.1) 0.6–0.8 | 0.6 (0.2) 0.2–1.0 |
| Sapling/shrub percent dead (%) | Average percent dead of surface fuel layer by volume | 9 (9) 0–36 | 8 (3) 4–11 | 23 (12) 4–48 |
| Sagebrush cover (%) | Percent cover of sagebrush species (<i>Artemisia</i> spp.) | — | — | 27 (16) 0–54 |

Note: Values are expressed as mean, with SD in parentheses, and range.

and mean homogeneity for each band. This resulted in a total of 10 lidar-derived predictors and 30 imagery-derived predictors.

Predicting fuels and structure with lidar-imagery fusion

We developed linear regression models for each vegetation structure and fuel metric (Table 2; Appendix S1: Table S2; Figure 2). We used exhaustive best subsets model selection to fit models to either all forest plots (conifer and deciduous, $n = 28$), conifer plots only ($n = 23$), or shrubland plots only ($n = 15$). The number of predictors for each model was limited to a maximum of five (forest or conifer models) or three (shrubland models) to minimize overfitting. Models were first assessed to confirm that they met assumptions of linearity based on residual plots and normality based on quantile–quantile plots, and dependent variables were transformed as needed to meet assumptions (Appendix S1:

Table S2). Models with strongly correlated predictors (Pearson's $|r| > 0.7$), multicollinearity assessed as variance inflation factor > 5 , or high influence of individual observations (Cook's distance $D > 1$) were excluded from consideration. We selected final models based on the lowest root-mean-squared-error from leave-one-out cross-validation.

Mapping fuels and structure

We used final regression models to project fuels and vegetation structure throughout the study region at 30-m resolution. We did not map areas managed or disturbed following acquisition of remotely sensed data in 2014. Some mapped values were unrealistic or far outside the range of field observations. These outlier values were set to either the natural minimum or maximum (e.g., 0% or 100% canopy cover) or twice the maximum value observed in the field. We compared final lidar-imagery fusion canopy fuels maps, as well

TABLE 2 Performance of best models for predicting structure and fuels

| Structure or fuels metric | Vegetation type(s) included in model | n | Adjusted R^2 | R^2 | RMSE | RMSEcv |
|---|--------------------------------------|----|----------------|-------|--------------|--------|
| Forest structure | | | | | | |
| Tree density (stems ha ⁻¹) | Conifer, deciduous | 28 | 0.72 | 0.77 | 0.45 (1419) | 0.57 |
| Tree basal area (m ² ha ⁻¹) | Conifer, deciduous | 28 | 0.84 | 0.86 | 0.52 (5.0) | 0.58 |
| Sapling density | Did not meet assumptions | — | — | — | — | — |
| Sapling height | Did not meet assumptions | — | — | — | — | — |
| Canopy fuel layer | | | | | | |
| Canopy cover (%) | Conifer, deciduous | 28 | 0.73 | 0.78 | 9 | 11 |
| Canopy height (m) | Conifer, deciduous | 28 | 0.94 | 0.95 | 1.6 | 2.0 |
| Canopy fuel load (kg m ⁻²) | Conifer | 23 | 0.88 | 0.90 | 0.09 (0.18) | 0.11 |
| Canopy bulk density (kg m ⁻³) | Conifer | 23 | 0.84 | 0.87 | 0.03 (0.020) | 0.04 |
| Canopy base height (m) | Conifer | 23 | 0.86 | 0.89 | 0.09 (0.1) | 0.12 |
| Surface fuel layer | | | | | | |
| Coarse woody debris cover (%) | Conifer | 23 | 0.65 | 0.73 | 4 | 4 |
| Coarse woody debris biomass (Mg ha ⁻¹) | Conifer | 23 | 0.65 | 0.73 | 0.38 (25.2) | 0.49 |
| Sapling/shrub cover (%) | Conifer | 23 | 0.79 | 0.84 | 5 | 7 |
| Sapling/shrub height (m) | Conifer | 23 | 0.55 | 0.65 | 0.2 | 0.3 |
| Sapling/shrub cover (%) | Shrubland | 15 | 0.57 | 0.66 | 10 | 13 |
| Sapling/shrub height (m) | Shrubland | 15 | 0.88 | 0.90 | 0.1 | 0.1 |
| Sapling/shrub percent dead | Shrubland | 15 | 0.89 | 0.92 | 0.15 (4) | 0.19 |
| Sagebrush cover (proportion of total sapling/shrub cover) | Shrubland | 15 | 0.90 | 0.92 | 0.09 | 0.11 |

Note: Values in parentheses are back-transformed RMSE, if applicable. For metrics that were transformed to meet model assumptions (see Appendix S1: Table S2), root-mean-squared error is also calculated from back-transformed predicted values. Note that the sagebrush cover model was fit to the proportion of sagebrush cover relative to total sapling/shrub cover.

Abbreviations: RMSE, root-mean-squared error; RMSEcv, root-mean-squared error of leave-one-out cross-validation.

as LANDFIRE fuels maps, with our field data (see Appendix S2).

Q1: How do fuels and burn severity compare in young versus mature subalpine forest?

Within the Berry Fire perimeter (Figure 1c), we identified areas of mature forest that had not previously burned for over 125 years using perimeter data from Grand Teton National Park (unpublished data) and Monitoring Trends in Burn Severity (MTBS; Eidenshink et al., 2007; MTBS Project, 2019). We compared mature forest fuels and burn severity with young, ~30-year-old forest that burned as stand-replacing fire in 1987 or 1988. We restricted comparison to areas that burned under similar fire weather (i.e., high fire spread days only; GeoMAC, 2016), were classified as conifer forest prior to the Berry Fire (Cogan et al., 2005), and were within GRTE. We quantified burn severity using relative difference normalized burn ratio (RdNBR; Miller & Thode, 2007; MTBS Project, 2019), which effectively characterizes field-measured burn severity in the region across a range of stand ages (Abendroth, 2008; Harvey, 2015; Saberi, 2019). We excluded RdNBR values that were likely unburned ($\text{RdNBR} < 0$) or anomalously high ($\text{RdNBR} > 2000$) and used a regionally calibrated threshold to delineate stand-replacing fire ($\text{RdNBR} > 675$; Harvey et al., 2016).

In both young and mature forest that burned in the Berry Fire, we randomly selected 30 points separated by >500 m to avoid spatial autocorrelation (Harvey et al., 2014, 2016). To strengthen inferences from these observational data, we used propensity score matching based on elevation and slope to exclude eight points, four each from young and mature forest, that fell outside overlapping ranges (Butsic et al., 2017). For remaining points (total $n = 52$), we obtained RdNBR from the closest 30-m resolution MTBS grid cell, and we used grid cell footprints to extract lidar and imagery predictors and calculate fuel loads (using equations from Appendix S1: Table S2). We compared forest structure, canopy and surface fuels, and burn severity between young and mature forests with two-sided Wilcoxon rank-sum tests.

Q2: How well do fuels predict burn severity under extreme versus moderate fire weather?

We assessed how well fuels and forest structure predicted burn severity within the full Berry Fire perimeter, including

all reburned areas (Figure 1c). We again used RdNBR (values between 0 and 2000) to quantify burn severity, excluded areas outside of GRTE, and only included areas classified as conifer forest or recently burned vegetation in the 2005 vegetation map. Areas were delineated as having burned under extreme fire weather (22 August, 23–24 August, and 11 September fire growth) or relatively moderate fire weather (all other days). For each fire weather condition, we randomly selected 50 points ($n = 100$ total) separated by >500 m and determined RdNBR and fuel loads as described above. We assigned approximate burn date based on fire progression maps (GeoMAC, 2016).

We fit separate linear mixed effects models to predict burn severity on either extreme or moderate weather days from forest structure and fuels as fixed effects and burn date as a random effect to account for daily variability in fire weather. We transformed fuels predictors to meet model assumptions (see Appendix S1: Table S2). For strongly correlated predictors (Pearson's $|r| > 0.7$), we retained the predictor hypothesized to directly affect burn severity or more strongly correlated with RdNBR. This resulted in basal area, canopy height, canopy cover, and CBD being excluded from model fitting. We then performed exhaustive model selection and selected the top models as those where all predictors were significant ($p < 0.05$) and Akaike information criterion corrected for small sample size (AIC_c) was within two of the best AIC_c model. We used residual and quantile-quantile plots to determine that models met assumptions, and model residuals were not spatially autocorrelated based on Moran's I . Model fit was assessed using variance explained by fixed effects (marginal $R^2_{\text{LMM(m)}}$) and by the full model (conditional $R^2_{\text{LMM(c)}}$; Nakagawa & Schielzeth, 2013).

All data processing, analysis, and map creation were performed using ArcGIS Desktop 10.6 (ESRI, Redlands, CA) and R Version 3.6.1 (R Core Team, 2019). We primarily relied on R packages ape (Paradis & Schliep, 2019), asbio (Aho, 2020), car (Fox & Weisberg, 2019), caret (Kuhn et al., 2019), corrplot (Wei & Simko, 2017), doParallel (Microsoft & Weston, 2019a), fasterize (Ross, 2018), foreach (Microsoft & Weston, 2019b), glcm (Zvoleff, 2020), leaps (Lumley & Miller, 2017), lidR (Roussel & Auty, 2019), lme4 (Bates et al., 2015), lmerTest (Kuznetsova et al., 2017), MatchIt (Ho et al., 2011), MuMIn (Barton, 2019), openxlsx (Schaubberger & Walker, 2019), optimx (Nash & Varadhan, 2011), qpcR (Spiess, 2018), raster (Hijmans, 2019), RColorBrewer (Neuwirth, 2014), rgdal (Bivand et al., 2019), rgeos (Bivand & Rundel, 2019), RSQLite (Muller et al., 2019), sf (Pebesma, 2018), sp (Pebesma & Bivand, 2005), tidyverse (Wickham et al., 2019), and tmap (Tennekes, 2018).

RESULTS

Predicting and mapping forest and shrubland structure and fuels

Predicting fuels and structure with lidar-imagery fusion

Lidar and imagery variables strongly predicted forest and shrubland structure and fuel metrics (R^2 from 0.65 to 0.95; Table 2, Figure 3; Appendix S1: Figure S1). Leave-one-out cross-validation RMSEs were between 11% and 38% higher than RMSEs for models fit to the full data set. Top-of-canopy metrics canopy height ($R^2 = 0.95$) and cover ($R^2 = 0.78$) generally had higher goodness-of-fit than surface fuel metrics with the exception of conifer forest sapling/shrub cover, which had a higher R^2 (0.84) than canopy cover. Models for stand basal area ($R^2 = 0.86$) and within-canopy fuel metrics (R^2 from 0.87 to 0.90) performed nearly as well as canopy height. Sapling/shrub height in conifer forests ($R^2 = 0.65$) and sapling/shrub cover in shrubland ($R^2 = 0.66$) had the poorest model fits. We did not predict sapling density or height because models did not meet linear regression assumptions.

Most top models included both lidar- and imagery-derived predictors (Appendix S1: Table S2). A lidar-derived metric generally had the highest predictive power for canopy fuel metrics, whereas an imagery-derived metric had the highest predictive power for all surface fuel metrics except sapling/shrub cover in shrublands. Final models for canopy base height and sapling/shrub percent dead included only imagery predictors. No top models included only lidar predictors.

Mapping fuels and structure

Mapped fuel and structure distributions aligned well with field data (Figure 4a,b; Appendix S1: Figures S2–S4). Histograms of mapped and observed data peaked at similar values, although field observations were sometimes bimodal or multimodal. Mapped canopy base heights skewed slightly taller than field observations, although in both cases most CBHs were short (<1 m height). Some metrics were reclassified to minimum or maximum bounds; this affected 5.7% of mapped values in forests and 14.0% of mapped values in shrublands (Appendix S1: Table S3). Proportion sagebrush in shrublands was most often outside of bounds (44.8% of values). Other metrics that more frequently (>5% of mapped values) exceeded either minimum or

maximum thresholds before reclassification were CWD biomass, CWD cover, sapling/shrub cover, and sapling/shrub height in conifer forests.

Maps of forest and shrubland structure and fuels captured expected patterns across much of the study landscape (Figure 4c,d; Appendix S1: Figures S5–S8). For example, areas within 2006 and 2009 fire perimeters had low canopy fuel loads and patches of high CWD cover and biomass. Shrubland was dominated by sagebrush at low, but not high, elevations. However, some predictions appeared erratic in locations that were less represented by field data. For example, at higher elevations and on steeper slopes within the rugged terrain of the Tetons, canopy and surface fuels were consistently predicted to be higher than the landscape average.

Q1: How do fuels and burn severity compare in young versus mature subalpine forest?

Young and mature forests that burned in the Berry Fire had similar canopy fuel load (median 1.33 and 1.27 kg m⁻², respectively, $p = 0.59$), canopy base height (0.6 m, $p = 0.19$), basal area (25.5 and 24.5 m² ha⁻¹, $p = 0.33$), CWD biomass (29.5 and 37.5 Mg ha⁻¹, $p = 0.12$), and sapling/shrub height (0.3 and 0.6 m, $p = 0.21$; Figure 5; Appendix S1: Figure S9). However, compared to mature forests, young forests had higher CBD (median 0.163 vs. 0.098 kg m⁻³, $p < 0.001$), canopy cover (67% vs. 47%, $p = 0.001$), tree density (5029 vs. 1761 trees ha⁻¹, $p < 0.001$), and CWD cover (11% vs. 8%, $p = 0.01$), but lower canopy height (14.5 vs. 24.5 m, $p < 0.001$) and sapling/shrub cover (13% vs. 26%, $p < 0.001$). Thus, across a similar range of canopy fuel loads, canopy fuels were much more densely packed in young compared to mature forests (Figure 5).

Young and mature forest burned at similar burn severity (median RdNBR 667 and 758, respectively, $p = 0.29$; Figure 6) on days of similar, extreme fire weather. At least half of the sampled grid cells burned as stand-replacing fire in both young and mature forests (RdNBR > 675).

Q2: How well do fuels predict burn severity under extreme versus moderate fire weather?

On days of extreme fire weather, higher burn severity was best predicted by higher tree density and sapling/shrub

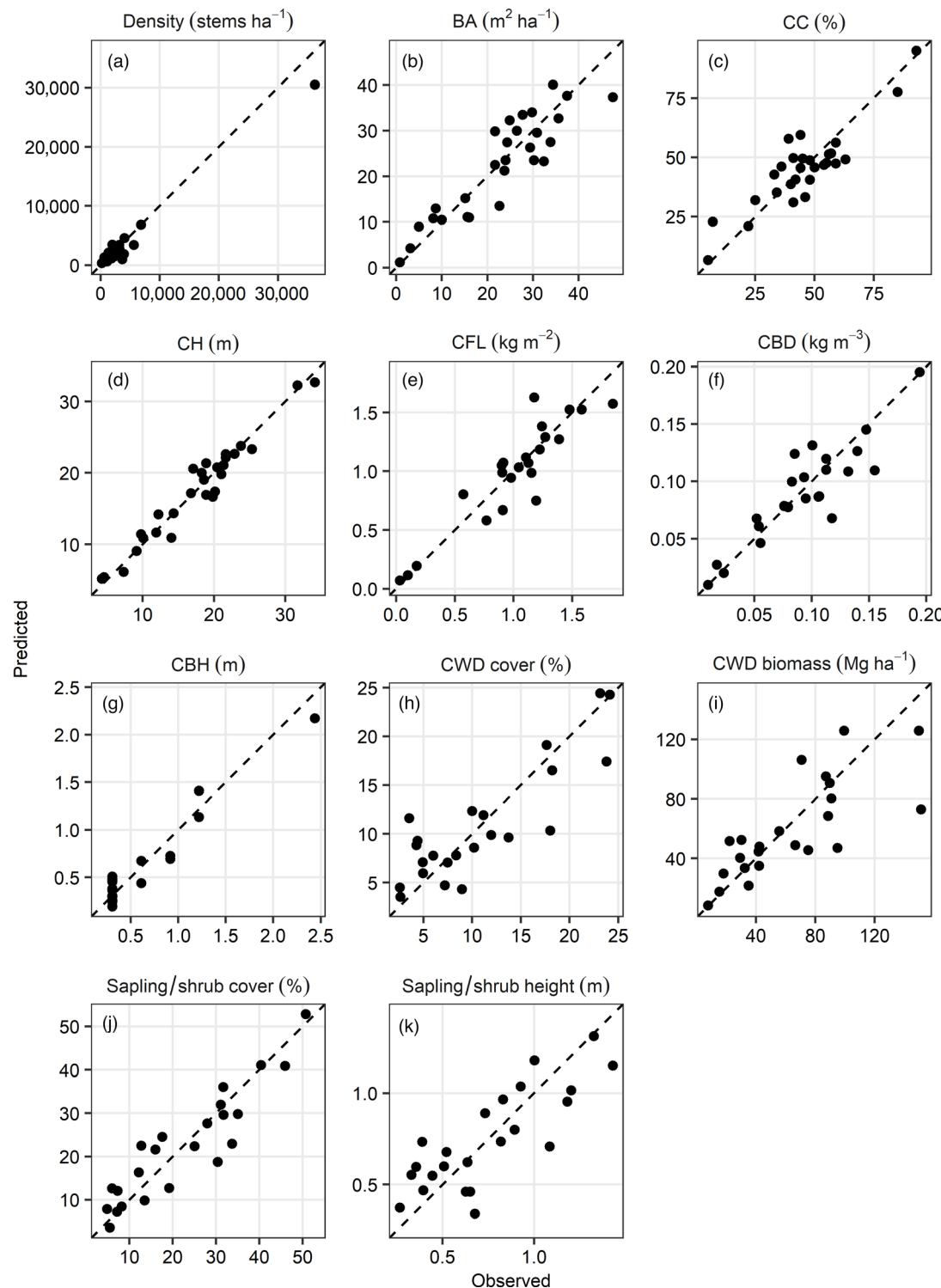


FIGURE 3 Predicted versus observed (field data) values for final forest structure and fuels regression models. Note that some models were fit to transformed values (see Appendix S1: Table S2). Dashed lines are 1:1 lines. (a–d) Models fit to combined conifer and deciduous plots ($n = 28$). (e–k) Models fit to conifer forest only ($n = 23$). BA, basal area; CBD, canopy bulk density; CBH, canopy base height; CC, canopy cover; CFL, canopy fuel load; CH, canopy height; CWD, coarse woody debris

cover, and burn date did not improve model fit (fixed effects marginal $R^2_{\text{LMM(m)}} = 0.27$ and full model conditional $R^2_{\text{LMM(c)}} = 0.27$; Table 3). On days of moderate fire

weather, higher burn severity was best predicted by higher coarse wood biomass, tree density, and sapling/shrub cover but with lower explanatory power ($R^2_{\text{LMM(m)}} = 0.15$ in top

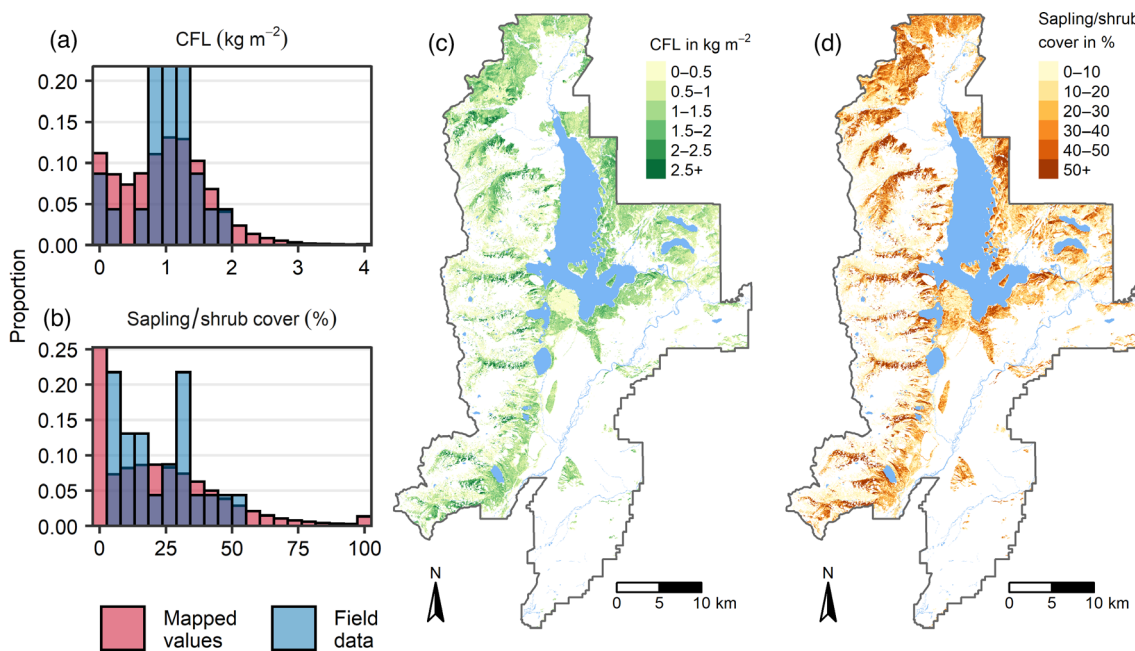


FIGURE 4 (a, b) Histograms showing distribution of mapped values ($n = 505,240$; blue) versus field data observations ($n = 23$, red) for canopy fuel load (CFL) and sapling/shrub cover in conifer forests. Overlapping areas are in purple. (c, d) Final lidar-imagery fusion fuels maps for canopy fuel load and sapling/shrub cover for conifer forests at 30-m resolution. Water is shown in blue.

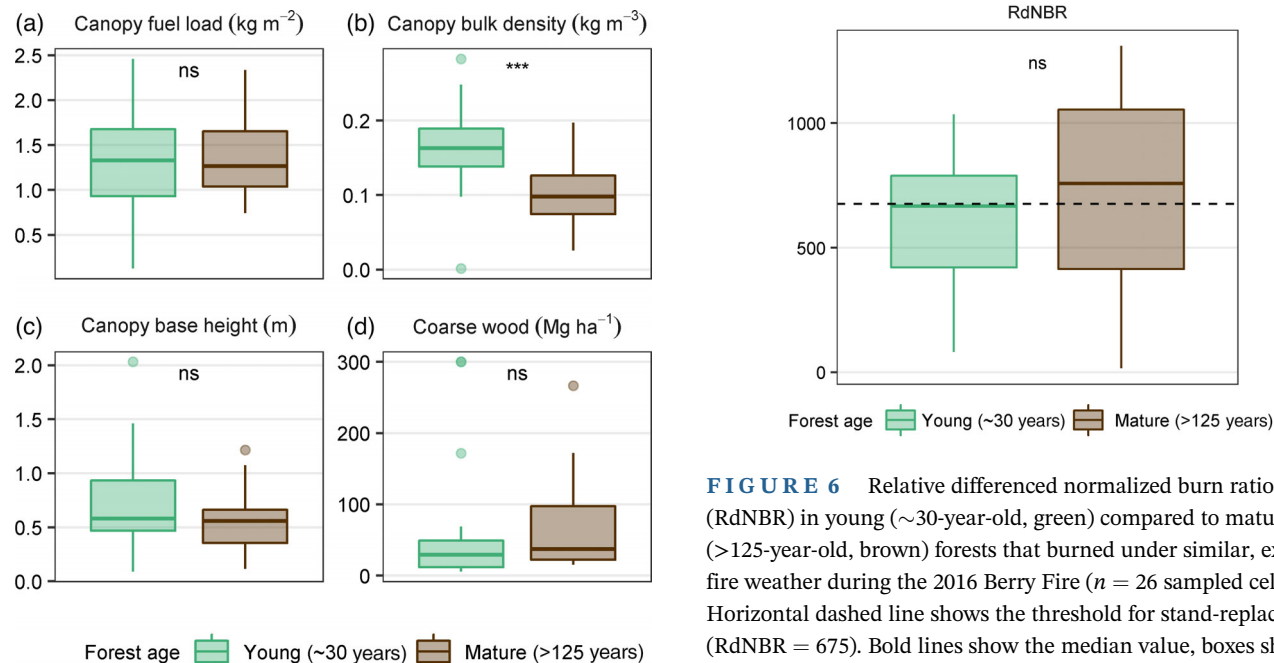


FIGURE 5 (a–c) Canopy and (d) surface fuels in young (~30-year-old, green) compared to mature (>125-year-old, brown) forests that burned during the 2016 Berry Fire ($n = 28$ sampled cells each). Bold lines show the median value, boxes show the interquartile range (IQR), and whiskers extend $1.5 \times$ IQR or to the most extreme data point. Results of Wilcoxon rank-sum tests indicate whether differences between distributions are not statistically significant (ns) or statistically significant at $p < 0.001$ (***)

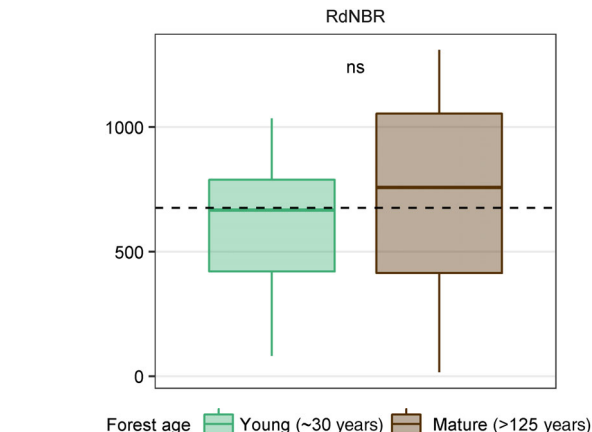


FIGURE 6 Relative differenced normalized burn ratio (RdNBR) in young (~30-year-old, green) compared to mature (>125-year-old, brown) forests that burned under similar, extreme fire weather during the 2016 Berry Fire ($n = 26$ sampled cells each). Horizontal dashed line shows the threshold for stand-replacing fire (RdNBR = 675). Bold lines show the median value, boxes show the interquartile range (IQR), and whiskers extend $1.5 \times$ IQR or to the most extreme data point. Results of Wilcoxon rank-sum tests indicate that differences between distributions are not statistically significant (ns).

model); burn date explained more variability and improved model fit ($R^2_{LMM(c)} = 0.51$ in top model). A second moderate fire weather model included only tree density ($R^2_{LMM(m)} = 0.06$, $R^2_{LMM(c)} = 0.46$).

TABLE 3 Linear mixed effects models predicting burn severity on extreme versus moderate fire weather days, including all top models within two AIC_c in which all predictors were significant ($p < 0.05$)

| Fire weather | AIC _c | R ² _{LMM(m)} | R ² _{LMM(c)} | Fixed effects | Estimate | t | p | Random effect |
|--------------|------------------|----------------------------------|----------------------------------|-------------------------|----------|--------|--------|---------------|
| Extreme | 743.9 | 0.27 | 0.27 | Intercept | -1368.8 | -2.482 | 0.02 | Burn date |
| | | | | Ln(Tree density) | 256.4 | 3.519 | <0.001 | |
| | | | | Sapling/shrub cover | 7.6 | 3.345 | 0.002 | |
| Moderate | 727.6 | 0.15 | 0.51 | Intercept | -915.5 | -2.275 | 0.03 | Burn date |
| | | | | Ln(Tree density) | 103.5 | 2.309 | 0.03 | |
| | | | | Ln(Coarse wood biomass) | 121.6 | 2.304 | 0.03 | |
| Moderate | 728.9 | 0.06 | 0.46 | Intercept | -307.4 | -0.877 | 0.39 | Burn date |
| | | | | Ln(Tree density) | 108.4 | 2.346 | 0.02 | |

Note: Variance explained is reported for fixed effects only (marginal R²_{LMM(m)}) and for the full mixed effects model (conditional R²_{LMM(c)}).

Abbreviation: AIC_c, Akaike information criterion corrected for small sample size.

DISCUSSION

Fusion of lidar and aerial imagery predicted canopy and surface fuels in a large fire-prone landscape with high accuracy across a wide range of woody vegetation structures. Although canopy metrics were generally predicted with highest accuracy, surface fuels, including downed coarse wood, were predicted surprisingly well. Using this fuels map to assess burn severity in a changing fire regime revealed that young (~30-year-old) postfire forests had abundant, densely packed canopy fuels and burned at similar severity as mature forests under similar weather conditions. Fuels were weak predictors of burn severity in the Berry Fire, which included a large proportion of short-interval reburn, but contrary to our hypothesis, fuels better predicted severity under extreme rather than moderate fire weather. Our findings are relevant for subalpine landscapes in the US Northern Rocky Mountains that are increasingly dominated by young, postfire lodgepole pine forests vulnerable to short-interval fire.

Lidar-imagery fusion effectively predicted and mapped vegetation structure and fuels

Lidar-imagery fusion models performed well and led to maps that appropriately represented spatial patterns and variability in vegetation structure and fuels throughout much of the study region. Lidar availability is increasing across the United States (NOAA, 2021), and we demonstrated that medium-resolution lidar (5.7 points m⁻²) can effectively characterize canopy and surface fuel metrics that are critically important for fire and resource managers. Ideally, field data should be collected within 1 year of

acquisition of remotely sensed data (Laes et al., 2011). However, we show that models can perform well despite a 5-year gap between lidar and field data collection in forests and shrublands where vegetation changes slowly in the absence of disturbance. Most top models included both lidar and imagery predictors, indicating that lidar and imagery were complementary and enhanced model performance. This is consistent with previous studies that found lidar-imagery fusion was superior to using either lidar or imagery predictors alone (Erdody & Moskal, 2010; Jakubowski et al., 2013; Mutlu et al., 2008).

As expected, fuel and structure metrics closer to the top of the canopy were generally predicted with higher accuracy than surface fuels. However, within-canopy and surface fuel layer predictions performed better than anticipated. For example, CWD cover and biomass were strongly predicted despite being well below and often obscured by the top of the forest canopy, which is important because CWD is highly variable and difficult to assess across subalpine forested landscapes (Tinker & Knight, 2000). Strong model predictions may be due to consistent patterns of forest and fuel succession in this region following stand-replacing disturbances. Coarse woody debris is high 10–20 years after severe fire and declines as forests recover, achieve canopy closure, and increase in height, but subsequently increases after 100–200 years as trees die and fall, creating gaps in the canopy (Kashian et al., 2013; Lotan et al., 1985; Romme, 1982). Similarly, CBH starts low, increases, and then declines as gaps enable growth of trees in the understory. As indirect proxies, predictors that characterize successional changes in total and within-plot variability in biomass or leaf area (e.g., NDVI; Jensen, 2007) or in height may be well suited to predict these within-canopy or surface fuel metrics (Pesonen et al., 2008).

Young and mature subalpine forests had similar fuel loads and burn severity

Young forests did not limit burn severity in the Berry Fire. As hypothesized, fuel loads and burn severity were similar or higher in young compared to mature subalpine forests that burned under similar fire weather. Our findings are consistent with rapid serotinous lodgepole pine regeneration and fuels recovery after stand-replacing fire in mature forests (Nelson et al., 2016; Turner et al., 2004). We found that young forests had low canopy base heights and high canopy bulk densities, which enable crown fire under extreme fire weather conditions (Nelson et al., 2017; Van Wagner, 1977, 1989). Fires can limit subsequent burn severity for over 20 years in some western US forests (Parks et al., 2014; Stevens-Rumann et al., 2016), and our results suggest that burn severity is limited for less than 30 years in lodgepole pine-dominated subalpine forests. Given the combination of abundant, densely packed canopy fuels close to the ground and high CWD cover and biomass, we might have expected even higher burn severity in young versus mature forest. Reburns where nearly all prefire biomass was consumed, including foliage, young trees, and CWD, were observed in the field in the Berry Fire (Turner et al., 2019). However, these higher severities may be poorly differentiated by remotely sensed indices of burn severity, which characterize canopy mortality well but are less able to detect variation in dead biomass consumption or surface burn severity (Saberi, 2019).

Understanding whether young forests will limit fire spread or severity is critical for anticipating fire behavior and forest recovery. Fire modelers update fuels maps based on expert knowledge of fire behavior and whether recent disturbances have altered fuels (Stratton, 2009). Our findings suggest that by 30 years postfire, subalpine lodgepole pine-dominated forests such as those prevalent throughout Greater Yellowstone can have similar fuel loads and even higher CBD compared to mature forests and should not be considered effective fire breaks, meaning they may neither slow fire spread nor reduce burn severity. This also has important implications for future forest landscapes, because severe short-interval fires can hamper subsequent forest recovery and initiate transitions to different forest types or nonforest vegetation (Coop et al., 2020; Enright et al., 2015; Prichard et al., 2017).

Forest structure and fuels predicted burn severity better on extreme weather days

Contrary to our hypothesis, forest structure and fuels better predicted burn severity under extreme versus moderate weather conditions. One possible explanation is that

burn severity is primarily detecting differences in canopy mortality due to crown fire. Under extreme fire weather, very low fuel moisture and high winds create the necessary conditions for crown fire initiation and spread (Renkin & Despain, 1992), but canopy fuel continuity may mediate fire effects. However, under moderate conditions with greater daily and potentially hourly variability in fire weather, the conditions for crown fire initiation and spread are less frequently met, and therefore, burn severity can be low even when fuels are abundant. It is nevertheless surprising that our results are contrary to the conventional wisdom that the relative importance of fuels is diminished under extreme fire weather in these forest types. It is important to note that we used daily fire progression maps, which are subject to error and uncertainty, as a proxy for moderate versus extreme fire weather. Fire risk assessments are often conducted based on worst-case weather scenarios, and our results indicate that prefire forest conditions can explain a small but meaningful amount of variation in potential fire effects on forests under extreme fire weather.

Surprisingly, canopy fuel metrics typically used to anticipate fire behavior (canopy fuel load, bulk density, and base height) were not included in top models. Instead, we found that tree density, sapling/shrub cover, and coarse wood biomass were the best predictors of burn severity. Although not strongly correlated in our study, higher tree densities were positively associated with higher canopy bulk densities and fuel loads, and horizontal continuity of canopy fuels increases with stand density. Sapling/shrub cover includes trees <2 m in height and thus quantifies ladder fuels, which enable surface fires to ignite the canopy, while high CWD biomass lengthens fire residence times and prolongs fuel consumption (Graham et al., 2004). Our analysis of the Berry Fire indicates significant but weak fuels effects on burn severity in a fire with a large proportion of reburned forest. Another recent study compared multiple fire hazard indices with burn severity in the Berry Fire and found that including canopy cover and surface fuel models mapped by LANDFIRE improved predictions of categorical burn severity, although relationships were still weak (Szpakowski et al., 2021). Our study supports the use of tree density, shrub cover, and coarse wood biomass as better predictors and provides new maps that can be incorporated into risk assessments. We further provide a benchmark that can be used to assess whether fuels more strongly regulate burn severity in future fires. It is important to note that our models did not include fine woody debris or herbaceous fuels, which we did not expect to be effectively characterized under a forest canopy by medium-resolution lidar. These fuels are often represented by categorical fuel models, but future studies should

explore methods for creating continuous fine surface fuels maps to further improve predicted fire behavior and effects.

Management applications for vegetation structure and fuels maps

Maps of vegetation structure and fuels can be used to support many management applications in combination with other geospatial data. For example, maps can be used in prefire planning to prioritize mechanical fuels treatment locations (North et al., 2015), to predict suppression difficulty under varying fire weather conditions (Rodríguez y Silva et al., 2014), or to identify and improve areas with relatively little vegetation to serve as firefighter safety zones (Dennison et al., 2014). Numerous studies have used lidar-derived data on vegetation structure to both understand and predict suitability of wildlife habitat (e.g., Garcia-Feced et al., 2011; Zhao et al., 2012). In Grand Teton National Park, resource managers and fire ecologists plan to test our map for quantifying the effectiveness of fuels treatments, monitoring fire effects, and mapping greater sage-grouse (*Centrocercus urophasianus*) habitat based on shrub height and sagebrush percent cover. If lidar is flown in future years, our regression models can be used to update the fuels map and assess landscape change.

Limitations and recommendations

The primary limitation of this study is that we were unable to perform an independent field-based validation of our fuels map. Therefore, we recommend that managers using either our fuels map or regression equations to predict fuels in other landscapes critically evaluate the reliability of mapped fuel metrics, ideally by using independent field observations to validate fuels predictions. In particular, values that were set to the minimum or maximum may not be representative of conditions on the ground. These values tend to occur at higher elevations and on steeper slopes and often coincide with forest edges (e.g., edge of forest and lake, edge of forest and road) and with higher proportions of nonvegetated surfaces (e.g., rocky or largely barren slopes). Variation in topographic conditions may affect the reliability of lidar predictor variables (Guo et al., 2010), whereas snow cover (present in some NAIP imagery at higher elevations) and shadows likely produce erroneous NAIP predictor values. Model precision (i.e., RMSE) should also be taken into consideration when using mapped values to plan management activities or make ecological interpretations.

Finally, we did not test how mechanical treatments or disturbance history might affect relationships between lidar and imagery predictors and fuel characteristics. Because the model for CBH only includes imagery predictors that do not penetrate the canopy, changes in CBH due to fuels treatments may not be well characterized by our models.

CONCLUSIONS

Quantifying forest fuels, and relationships between fuels and burn severity, is increasingly important for understanding how forest landscapes and fire behavior may change as fires recur more frequently. Here, we show that lidar–imagery fusion can accurately predict fuels across large landscapes, and fuels maps can improve understanding of how fuels affect burn severity. Although we found only weak evidence of fuels limiting burn severity in a single short (<30-year)-interval reburn, postfire fuel loads and forest recovery are likely to differ after short- compared to long-interval stand-replacing fire. As fire frequency increases, landscape-scale fuel loads and continuity in subalpine forests may decline to the point where they are no longer capable of sustaining large patches of high-severity fire (Braziunas et al., 2021; Hansen et al., 2020). Fire managers should continually reassess and update expectations about fire behavior in future forest landscapes. For now, however, our results suggest that young subalpine forests in the Northern Rocky Mountains have sufficient fuel loads to burn at high severity and should not be considered effective fire breaks.

AUTHOR CONTRIBUTIONS

Kristin H. Braziunas, Diane C. Abendroth, and Monica G. Turner designed the study; Kristin H. Braziunas led data collection and analysis with support from Diane C. Abendroth and Monica G. Turner; and Kristin H. Braziunas wrote the manuscript with contributions from Diane C. Abendroth and Monica G. Turner.

ACKNOWLEDGMENTS

We thank Windy Bunn, Chip Collins, Jacob Henrie, and Eric Neiswanger for their input during our initial project overview presentation at Grand Teton National Park headquarters. We are especially grateful to the many individuals who assisted with field data collection, including Paul Boehlein, Olivia Burke, Claire Finucane, Nathan Kiel, Ray Lopez, Kate Patronik, Trond Simensen, Drew Smith, Ron Steffens, and Jill Stephenson. We also thank Todd Erdody, Anu Kramer, Chris Kucharik, Tyler Hoecker, Anthony Ives, Volker Radeloff, Adena Rissman,

Kyle Rodman, and two anonymous reviewers for providing constructive comments and/or technical assistance that greatly improved our study design and manuscript. We acknowledge funding from National Park Service Fuels Reserve Fund (National Park Service Task Agreement P17AC01466) and the University of Wisconsin Vilas Trust. Kristin H. Braziunas acknowledges support from a P.E.O. Ventura Neale Trust Endowed Scholar Award.

CONFLICT OF INTEREST

The authors declare no conflict of interest.

DATA AVAILABILITY STATEMENT

Data and code (Braziunas et al., 2022) are available from the Environmental Data Initiative: <https://doi.org/10.6073/pasta/4f6864a8c7bb0f712d0443fb334c73e>.

ORCID

Kristin H. Braziunas  <https://orcid.org/0000-0001-5350-8463>

Monica G. Turner  <https://orcid.org/0000-0003-1903-2822>

REFERENCES

- Abatzoglou, J. T., and A. P. Williams. 2016. “Impact of Anthropogenic Climate Change on Wildfire across Western US Forests.” *Proceedings of the National Academy of Sciences* 113: 11770–5.
- Abendroth, D. C. 2008. “Canopy Mortality Modeling and Mapping in Burned Areas of Northwest Wyoming.” MS thesis, Colorado State University.
- Aho, K. 2020. *asbio*: A Collection of Statistical Tools for Biologists. R package version 1.6-3. <https://CRAN.R-project.org/package=asbio>.
- Andersen, H. E., R. J. McGaughey, and S. E. Reutebuch. 2005. “Estimating Forest Canopy Fuel Parameters Using Lidar Data.” *Remote Sensing of Environment* 94: 441–9.
- Baker, W. L. 2002. “Indians and Fire in the U.S. Rocky Mountains: The Wilderness Hypothesis Renewed.” In *Fire, Native Peoples, and the Natural Landscape*, edited by T. R. Vale, 41–76. Washington, DC: Island Press.
- Baker, W. L. 2009. *Fire Ecology in Rocky Mountain Landscapes*. Washington, DC: Island Press.
- Balch, J. K., B. A. Bradley, J. T. Abatzoglou, R. C. Nagy, E. J. Fusco, and A. L. Mahood. 2017. “Human-Started Wildfires Expand the Fire Niche across the United States.” *Proceedings of the National Academy of Sciences* 114: 2946–51.
- Barton, K. 2019. *MuMIn*: Multi-Model Inference. R package version 1.43.15. <https://CRAN.R-project.org/package=MuMIn>.
- Bates, D., M. Mächler, B. M. Bolker, and S. C. Walker. 2015. “Fitting Linear Mixed-Effects Models Using lme4.” *Journal of Statistical Software* 67: 1–48.
- Bessie, W. C., and E. A. Johnson. 1995. “The Relative Importance of Fuels and Weather on Fire Behavior in Subalpine Forests.” *Ecology* 76: 747–62.
- Bigler, C., D. Kulakowski, and T. T. Veblen. 2005. “Multiple Disturbance Interactions and Drought Influence Fire Severity in Rocky Mountain Subalpine Forests.” *Ecology* 86: 3018–29.
- Bivand, R., T. Keitt, and B. Rowlingson. 2019. *rgdal*: Bindings for the “Geospatial” Data Abstraction Library. R package version 1.4-4. <https://CRAN.R-project.org/package=rgdal>.
- Bivand, R., and C. Rundel. 2019. *rgeos*: Interface to Geometry Engine – Open Source (‘GEOS’). R package version 0.5-1. <https://CRAN.R-project.org/package=rgeos>.
- Blanchard, S. D., M. K. Jakubowski, and M. Kelly. 2011. “Object-Based Image Analysis of Downed Logs in Disturbed Forested Landscapes Using Lidar.” *Remote Sensing* 3: 2420–39.
- Booz Allen Hamilton (BAH). 2015. *2014 Quadrennial Fire Review: Final Report*. Washington, DC: USDA Forest Service, Fire and Aviation Management, USDI Office of Wildland Fire.
- Brandegee, T. S. 1898. *Teton Forest Reserve and Southern Part of Yellowstone Park Forest Reserve*. US Geological Survey Nineteenth Annual Report Part V, PL. XLIII.
- Braziunas, K. H., W. D. Hansen, R. Seidl, W. Rammer, and M. G. Turner. 2018. “Looking beyond the Mean: Drivers of Variability in Postfire Stand Development of Conifers in Greater Yellowstone.” *Forest Ecology and Management* 430: 460–71.
- Braziunas, K. H., R. Seidl, W. Rammer, and M. G. Turner. 2021. “Can We Manage a Future with More Fire? Effectiveness of Defensible Space Treatment Depends on Housing Amount and Configuration.” *Landscape Ecology* 36: 309–30.
- Braziunas, K. H., M. G. Turner, and D. C. Abendroth. 2022. “Young Forests and Fire: Using Lidar-Imagery Fusion to Explore Fuels and Burn Severity in a Subalpine Forest Reburn, Grand Teton National Park, Wyoming. Version 1.” Environmental Data Initiative. <https://doi.org/10.6073/pasta/4f6864a8c7bb0f712d0443fb334c73e>.
- Brown, J. K. 1974. *Handbook for Inventorying Downed Woody Material*. Ogden, UT: USDA Forest Service, Intermountain Forest and Range Experiment Station, General Technical Report INT-16.
- Buma, B., S. Weiss, K. Hayes, and M. Lucash. 2020. “Wildland Fire Reburning Trends across the US West Suggest Only Short-Term Negative Feedback and Differing Climatic Effects.” *Environmental Research Letters* 15: 034026.
- Burns, R. M., and B. H. Honkala. 1990. “Silvics of North America.” In *Volume 1: Conifers*, edited by R. M. Burns and B. H. Honkala. Washington, DC: USDA Forest Service, Agriculture Handbook 654.
- Butsic, V., D. J. Lewis, V. C. Radloff, M. Baumann, and T. Kuemmerle. 2017. “Quasi-Experimental Methods Enable Stronger Inferences from Observational Data in Ecology.” *Basic and Applied Ecology* 19: 1–10.
- Calkin, D. E., M. P. Thompson, M. A. Finney, and K. D. Hyde. 2011. “A Real-Time Risk Assessment Tool Supporting Wildland Fire Decisionmaking.” *Journal of Forestry* 109: 274–80.
- Campbell, M. J., P. E. Dennison, and B. W. Butler. 2017. “A Lidar-Based Analysis of the Effects of Slope, Vegetation Density, and Ground Surface Roughness on Travel Rates for Wildland Firefighter Escape Route Mapping.” *International Journal of Wildland Fire* 26: 884–95.
- Cansler, C. A., and D. McKenzie. 2014. “Climate, Fire Size, and Biophysical Setting Control Fire Severity and Spatial Pattern in

- the Northern Cascade Range, USA.” *Ecological Applications* 24: 1037–56.
- Chamberlain, C. P., A. J. Sánchez Meador, and A. E. Thode. 2021. “Airborne Lidar Provides Reliable Estimates of Canopy Base Height and Canopy Bulk Density in Southwestern Ponderosa Pine Forests.” *Forest Ecology and Management* 481: 118695.
- Cogan, D., K. Varga, G. Kittel, K. McCloskey, D. Abendroth, J. Gremer, and C. Bolen. 2005. *USGS-NPS Vegetation Mapping Program: Grand Teton National Park and John D. Rockefeller, Jr. Memorial Parkway Final Project Report*. Denver, CO: USDI Bureau of Reclamation Technical Memorandum 8260-06-02.
- Collins, L., A. F. Bennett, S. W. J. Leonard, and T. D. Penman. 2019. “Wildfire Refugia in Forests: Severe Fire Weather and Drought Mute the Influence of Topography and Fuel Age.” *Global Change Biology* 25: 3829–43.
- Coop, J. D., S. A. Parks, C. S. Stevens-Rumann, S. D. Crausbay, P. E. Higuera, M. D. Hurteau, A. Tepley, et al. 2020. “Wildfire-Driven Forest Conversion in Western North American Landscapes.” *Bioscience* 70: 659–73.
- Coulloudon, B., K. Eshelman, J. Gianola, N. Habich, L. Hughes, C. Johnson, M. Pellatt, et al. 1999. *Sampling Vegetation Attributes*. Denver, CO: USDA Forest Service, USDI Bureau of Land Management, Technical Reference 1734-4.
- Dennison, P. E., G. K. Fryer, and T. J. Cova. 2014. “Identification of Firefighter Safety Zones Using Lidar.” *Environmental Modelling and Software* 59: 91–7.
- Despain, D. G., and R. E. Sellers. 1977. “Natural Fire in Yellowstone National Park.” *Western Wildlands* 4: 20–4.
- Dixon, G. E. 2002. *Essential FVS: A User’s Guide to the Forest Vegetation Simulator*. Fort Collins, CO: USDA Forest Service, Forest Management Service Center. (Revised 2015).
- Eidenshink, J., B. Schwind, K. Brewer, Z.-L. Zhu, B. Quayle, and S. Howard. 2007. “A Project for Monitoring Trends in Burn Severity.” *Fire Ecology* 3: 3–21.
- Engelstad, P. S., M. Falkowski, P. Wolter, A. Poznanovic, and P. Johnson. 2019. “Estimating Canopy Fuel Attributes from Low-Density Lidar.” *Fire* 2: 1–19.
- Enright, N. J., J. B. Fontaine, D. M. J. S. Bowman, R. A. Bradstock, and R. J. Williams. 2015. “Interval Squeeze: Altered Fire Regimes and Demographic Responses Interact to Threaten Woody Species Persistence as Climate Changes.” *Frontiers in Ecology and the Environment* 13: 265–72.
- Erdody, T. L., and L. M. Moskal. 2010. “Fusion of Lidar and Imagery for Estimating Forest Canopy Fuels.” *Remote Sensing of Environment* 114: 725–37.
- Fox, J., and S. Weisberg. 2019. *An R Companion to Applied Regression*, 3rd ed. Thousand Oaks, CA: Sage.
- Garcia-Feced, C., D. J. Tempel, and M. Kelly. 2011. “Lidar as a Tool to Characterize Wildlife Habitat: California Spotted Owl Nesting Habitat as an Example.” *Journal of Forestry* 109: 436–43.
- Geospatial Multi-Agency Coordination (GeoMAC). 2016. Berry Fire perimeter archive. https://gec.cr.usgs.gov/outgoing/GeoMAC/2016_fire_data/Wyoming/Berry/.
- Graham, R. T., S. McCaffrey, and T. B. Jain. 2004. *Science Basis for Changing Forest Structure to Modify Wildfire Behavior and Severity*. Fort Collins, CO: USDA Forest Service, Rocky Mountain Research Station, General Technical Report RMRS-GTR-120.
- Grand Teton National Park (GRTE). 2009. *Grand Teton National Park Fire Management Plan*. Washington, DC: National Park Service, US Department of the Interior.
- Guo, Q., W. Li, H. Yu, and O. Alvarez. 2010. “Effects of Topographic Variability and Lidar Sampling Density on Several DEM Interpolation Methods.” *Photogrammetric Engineering & Remote Sensing* 76: 701–12.
- Halofsky, J. E., D. L. Peterson, and B. J. Harvey. 2020. “Changing Wildfire, Changing Forests: The Effects of Climate Change on Fire Regimes and Vegetation in the Pacific Northwest, USA.” *Fire Ecology* 16: 4.
- Hansen, W. D., D. Abendroth, W. Rammer, R. Seidl, and M. G. Turner. 2020. “Can Wildland Fire Management Alter 21st-Century Subalpine Fire and Forests in Grand Teton National Park, Wyoming, USA?” *Ecological Applications* 30: e02030.
- Harmon, M. E., J. F. Franklin, F. J. Swanson, P. Sollins, S. V. Gregory, J. D. Lattin, N. H. Anderson, et al. 1986. “Ecology of Coarse Woody Debris in Temperate Ecosystems.” In *Advances in Ecological Research*, edited by A. MacFadyen and E. D. Ford, 133–302. Orlando, FL: Academic Press.
- Harvey, B. J. 2015. “Causes and Consequences of Spatial Patterns of Fire Severity in Northern Rocky Mountain Forests: The Role of Disturbance Interactions and Changing Climate.” PhD dissertation, University of Wisconsin-Madison.
- Harvey, B. J., D. C. Donato, W. H. Romme, and M. G. Turner. 2014. “Fire Severity and Tree Regeneration Following Bark Beetle Outbreaks: The Role of Outbreak Stage and Burning Conditions.” *Ecological Applications* 24: 1608–25.
- Harvey, B. J., D. C. Donato, and M. G. Turner. 2016. “Burn Me Twice, Shame on Who? Interactions between Successive Forest Fires across a Temperate Mountain Region.” *Ecology* 97: 2272–82.
- Hessburg, P. F., C. L. Miller, S. A. Parks, N. A. Povak, A. H. Taylor, P. E. Higuera, S. J. Prichard, et al. 2019. “Climate, Environment, and Disturbance History Govern Resilience of Western North American Forests.” *Frontiers in Ecology and Evolution* 7: 239.
- Higuera, P. E., and J. T. Abatzoglou. 2021. “Record-Setting Climate Enabled the Extraordinary 2020 Fire Season in the Western United States.” *Global Change Biology* 27: 1–2.
- Higuera, P. E., C. Whitlock, and J. A. Gage. 2011. “Linking Tree-Ring and Sediment-Charcoal Records to Reconstruct Fire Occurrence and Area Burned in Subalpine Forests of Yellowstone National Park, USA.” *Holocene* 21: 327–41.
- Hijmans, R. J. 2019. raster: Geographic Data Analysis and Modeling. R package version 3.0-2. <https://CRAN.R-project.org/package=raster>.
- Ho, D. E., K. Imai, G. King, and E. A. Stuart. 2011. “MatchIt: Non-parametric Preprocessing for Parametric Causal Inference.” *Journal of Statistical Software* 42: 1–28.
- Hyde, J., E. K. Strand, A. T. Hudak, and D. Hamilton. 2015. “A Case Study Comparison of LANDFIRE Fuel Loading and Emissions Generation on a Mixed Conifer Forest in Northern Idaho, USA.” *Fire Ecology* 11: 108–27.
- Jakubowski, M. K., Q. Guo, B. Collins, S. Stephens, and M. Kelly. 2013. “Predicting Surface Fuel Models and Fuel Metrics Using Lidar and CIR Imagery in a Dense, Mountainous Forest.” *Photogrammetric Engineering and Remote Sensing* 79: 37–49.

- Jensen, J. R. 2007. *Remote Sensing of the Environment: An Earth Resource Perspective*, 2nd ed. Upper Saddle River, NJ: Pearson Prentice Hall.
- Joyce, M. J., J. D. Erb, B. A. Sampson, and R. A. Moen. 2019. "Detection of Coarse Woody Debris Using Airborne Light Detection and Ranging (Lidar)." *Forest Ecology and Management* 433: 678–89.
- Kashian, D. M., W. H. Romme, D. B. Tinker, and M. G. Turner. 2013. "Postfire Changes in Forest Carbon Storage over a 300-Year Chronosequence of *Pinus contorta*-Dominated Forests." *Ecological Monographs* 83: 49–66.
- Keane, R. E. 2015. *Wildland Fuel Fundamentals and Applications*. New York, NY: Springer.
- Keane, R. E., T. Frescino, M. C. Reeves, and J. L. Long. 2006. "Mapping Wildland Fuel across Large Regions for the LANDFIRE Prototype Project." In *The LANDFIRE Prototype Project: Nationally Consistent and Locally Relevant Geospatial Data for Wildland Fire Management* 367–96. Fort Collins, CO: USDA Forest Service, Rocky Mountain Research Station, General Technical Report RMRS-GTR-175.
- Keane, R. E., K. Gray, and V. Bacciu. 2012. *Spatial Variability of Wildland Fuel Characteristics in Northern Rocky Mountain Ecosystems*. Fort Collins, CO: USDA Forest Service, Rocky Mountain Research Station, Research Paper RMRS-RP-98.
- Keane, R. E., J. M. Herynk, C. Toney, S. P. Urbanski, D. C. Lutes, and R. D. Ottmar. 2013. "Evaluating the Performance and Mapping of Three Fuel Classification Systems Using Forest Inventory and Analysis Surface Fuel Measurements." *Forest Ecology and Management* 305: 248–63.
- Keyser, C. E., and G. E. Dixon. 2008. *Tetons (TT) Variant Overview: Forest Vegetation Simulator*. Fort Collins, CO: USDA Forest Service, Forest Management Service Center.
- Knight, D. H., G. P. Jones, W. A. Reiners, and W. H. Romme. 2014. *Mountains and Plains: The Ecology of Wyoming Landscapes*, 2nd ed. New Haven, CT: Yale University Press.
- Krasnow, K., T. Schoennagel, and T. T. Veblen. 2009. "Forest Fuel Mapping and Evaluation of LANDFIRE Fuel Maps in Boulder County, Colorado, USA." *Forest Ecology and Management* 257: 1603–12.
- Kuhn, M., J. Wing, S. Weston, A. Williams, C. Keefer, A. Engelhardt, T. Cooper, et al. 2019. caret: Classification and Regression Training. R package version 6.0-84. <https://CRAN.R-project.org/package=caret>.
- Kuznetsova, A., P. B. Brockhoff, and R. H. B. Christensen. 2017. "lmerTest Package: Tests in Linear Mixed Effects Models." *Journal of Statistical Software* 82: 1–26.
- Laes, D., S. E. Reutebuch, R. J. McGaughey, and B. Mitchell. 2011. *Guidelines to Estimate Forest Inventory Parameters from Lidar and Field Plot Data*. Corvallis, OR: USDA Forest Service, Pacific Northwest Research Station.
- Lefsky, M. A., W. B. Cohen, G. G. Parker, and D. J. Harding. 2002. "Lidar Remote Sensing for Ecosystem Studies." *Bioscience* 52: 19.
- Lepczyk, C. A., L. M. Wedding, G. P. Asner, S. J. Pittman, T. Goulden, M. A. Linderman, J. Gang, and R. Wright. 2021. "Advancing Landscape and Seascape Ecology from a 2D to a 3D Science." *Bioscience* 71: 596–608.
- Loope, L. L., and G. E. Gruell. 1973. "The Ecological Role of Fire in the Jackson Hole Area, Northwestern Wyoming." *Quaternary Research* 3: 425–43.
- Loope, L. L., and R. P. Wood. 1976. "Fire Management in Grand Teton National Park." In *Proceedings of the Tall Timbers Fire Ecology Conference and Intermountain Fire Research and Land Management Symposium, Missoula, MT* 87–98. Tallahassee, FL: Tall Timbers Research Station.
- Lotan, J. E., J. K. Brown, and L. F. Neuenschwander. 1985. "Role of Fire in Lodgepole Pine Forests." In *Lodgepole Pine the Species and Its Management Symposium Proceedings*, edited by D. M. Baumgartner, et al., 133–52. Pullman, WA: Washington State University.
- Lumley, T., and A. Miller. 2017. leaps: Regression Subset Selection. R package version 3.0. <https://CRAN.R-project.org/package=leaps>.
- McKenzie, D., C. Miller, and D. A. Falk. 2011. "Toward a Theory of Landscape Fire." In *The Landscape Ecology of Fire*, edited by D. McKenzie, C. Miller, and D. A. Falk, 3–25. New York, NY: Springer Science & Business Media.
- Meigs, G. W., C. J. Dunn, S. A. Parks, and M. A. Krawchuk. 2020. "Influence of Topography and Fuels on Fire Refugia Probability under Varying Fire Weather Conditions in Forests of the Pacific Northwest, USA." *Canadian Journal of Forest Research* 50: 636–47.
- Meyer, M. D., S. L. Roberts, R. Wills, M. Brooks, and E. M. Winford. 2015. "Principles of Effective USA Federal Fire Management Plans." *Fire Ecology* 11: 59–83.
- Microsoft and S. Weston. 2019a. doParallel: Foreach Parallel Adapter for the "Parallel" Package. R package version 1.0.15. <https://CRAN.R-project.org/package=doParallel>.
- Microsoft and S. Weston. 2019b. foreach: Provides Foreach Looping Construct. R package version 1.4.7. <https://CRAN.R-project.org/package=foreach>.
- Miller, J. D., and A. E. Thode. 2007. "Quantifying Burn Severity in a Heterogeneous Landscape with a Relative Version of the Delta Normalized Burn Ratio (dNBR)." *Remote Sensing of Environment* 109: 66–80.
- Mitchell, B., M. Walterman, T. Mellin, C. Wilcox, A. M. Lynch, J. Anhold, D. A. Falk, et al. 2012. *Mapping Vegetation Structure in the Pinaleno Mountains Using Lidar. Phase 3: Forest Inventory Modeling*. Salt Lake City, UT: USDA Forest Service, Remote Sensing Applications Center RSAC-10007-RPT1.
- Moran, C. J., V. R. Kane, and C. A. Seielstad. 2020. "Mapping Forest Canopy Fuels in the Western United States with Lidar-Landsat Covariance." *Remote Sensing* 12: 1000.
- Moskal, L. M., and S. E. Franklin. 2002. "Multi-Layer Forest Stand Discrimination with Spatial Co-Occurrence Texture Analysis of High Spatial Detail Airborne Imagery." *Geocarto International* 17: 55–68.
- MTBS Project. 2019. MTBS Data Access: Fire Level Geospatial Data. USDA Forest Service/US Geological Survey. <http://mtbs.gov/direct-download>.
- Muller, K., H. Wickham, D. A. James, and S. Falcon. 2019. RSQLite: "SQLite" Interface for R. R package version 2.1.2. <https://CRAN.R-project.org/package=RSQLite>.
- Mutlu, M., S. C. Popescu, C. Stripling, and T. Spencer. 2008. "Mapping Surface Fuel Models Using Lidar and Multispectral Data Fusion for Fire Behavior." *Remote Sensing of Environment* 112: 274–85.
- NAIP. 2015. *National Agriculture Imagery Program*. Salt Lake City, UT: USDA Farm Service Agency.

- Nakagawa, S., and H. Schielzeth. 2013. "A General and Simple Method for Obtaining R² from Generalized Linear Mixed-Effects Models." *Methods in Ecology and Evolution* 4: 133–42.
- Nash, J. C., and R. Varadhan. 2011. "Unifying Optimization Algorithms to Aid Software System Users: Optimx for R." *Journal of Statistical Software* 43: 1–14.
- National Oceanic and Atmospheric Administration (NOAA) Office of Coastal Management. 2021. United States Interagency Elevation Inventory (USIEI). <https://coast.noaa.gov/inventory/>.
- Native Land Digital. 2021. Native Land Map. <https://native-land.ca/>.
- Nelson, K. N., M. G. Turner, W. H. Romme, and D. B. Tinker. 2016. "Landscape Variation in Tree Regeneration and Snag Fall Drive Fuel Loads in 24-Year Old Post-Fire Lodgepole Pine Forests." *Ecological Applications* 26: 2422–36.
- Nelson, K. N., M. G. Turner, W. H. Romme, and D. B. Tinker. 2017. "Simulated Fire Behaviour in Young, Postfire Lodgepole Pine Forests." *International Journal of Wildland Fire* 26: 852–65.
- Neuwirth, E. 2014. RColorBrewer: ColorBrewer Palettes. R package version 1.1-2. <https://CRAN.R-project.org/package=RColorBrewer>.
- North, M. P., A. Brough, J. W. Long, B. Collins, P. Bowden, D. Yasuda, J. Miller, and N. G. Sugihara. 2015. "Constraints on Mechanized Treatment Significantly Limit Mechanical Fuels Reduction Extent in the Sierra Nevada." *Journal of Forestry* 113: 40–8.
- O'Connor, C., M. Thompson, and F. Rodríguez y Silva. 2016. "Getting Ahead of the Wildfire Problem: Quantifying and Mapping Management Challenges and Opportunities." *Geosciences* 6: 35.
- Paradis, E., and K. Schliep. 2019. "Ape 5.0: An Environment for Modern Phylogenetics and Evolutionary Analyses in R." *Bioinformatics* 35: 526–8.
- Parks, S. A., L. M. Holsinger, C. Miller, and C. R. Nelson. 2015. "Wildland Fire as a Self-Regulating Mechanism: The Role of Previous Burns and Weather in Limiting Fire Progression." *Ecological Applications* 25: 1478–92.
- Parks, S. A., L. M. Holsinger, M. H. Panunto, W. M. Jolly, S. Z. Dobrowski, and G. K. Dillon. 2018. "High-Severity Fire: Evaluating Its Key Drivers and Mapping Its Probability across Western US Forests." *Environmental Research Letters* 13: 044037.
- Parks, S. A., C. Miller, C. R. Nelson, and Z. A. Holden. 2014. "Previous Fires Moderate Burn Severity of Subsequent Wildland Fires in Two Large Western US Wilderness Areas." *Ecosystems* 17: 29–42.
- Pebesma, E. 2018. "Simple Features for R: Standardized Support for Spatial Vector Data." *R Journal* 10: 439–46.
- Pebesma, E. J., and R. S. Bivand. 2005. Classes and Methods for Spatial Data in {R}. R News 5.
- Pesonen, A., M. Maltamo, K. Eerikäinen, and P. Packalèn. 2008. "Airborne Laser Scanning-Based Prediction of Coarse Woody Debris Volumes in a Conservation Area." *Forest Ecology and Management* 255: 3288–96.
- Prichard, S. J., C. S. Stevens-Rumann, and P. F. Hessburg. 2017. "Tamm Review: Shifting Global Fire Regimes: Lessons from Reburns and Research Needs." *Forest Ecology and Management* 396: 217–33.
- R Core Team. 2019. *R: A Language and Environment for Statistical Computing*. Vienna, Austria: R Foundation for Statistical Computing.
- Radeloff, V. C., D. P. Helmers, H. A. Kramer, M. H. Mockrin, P. M. Alexandre, A. Bar-Massada, V. Butsic, et al. 2018. "Rapid Growth of the US Wildland-Urban Interface Raises Wildfire Risk." *Proceedings of the National Academy of Sciences* 115: 3314–9.
- Rebain, S. 2010. *The Fire and Fuels Extension to the Forest Vegetation Simulator: Updated Model Documentation*. Fort Collins, CO: USDA Forest Service, Forest Management Service Center.
- Reeves, M. C., K. C. Ryan, M. G. Rollins, and T. G. Thompson. 2009. "Spatial Fuel Data Products of the LANDFIRE Project." *International Journal of Wildland Fire* 18: 250–67.
- Renkin, R. A., and D. G. Despain. 1992. "Fuel Moisture, Forest Type, and Lightning-Caused Fire in Yellowstone National Park." *Canadian Journal of Forest Research* 22: 37–45.
- Rodríguez y Silva, F., J. R. M. Martínez, and A. González-Cabán. 2014. "A Methodology for Determining Operational Priorities for Prevention and Suppression of Wildland Fires." *International Journal of Wildland Fire* 23: 544–54.
- Romme, W. 1982. "Fire and Landscape Diversity in Subalpine Forests of Yellowstone National Park." *Ecological Monographs* 52: 199–221.
- Romme, W. H., and D. G. Despain. 1989. "Historical Perspective on the Yellowstone Fires of 1988." *Bioscience* 39: 695–9.
- Ross, N. 2018. fasterize: Fast Polygon to Raster Conversion. R package version 1.0.0. <https://CRAN.R-project.org/package=fasterize>.
- Roussel, J.-R., and D. Auty. 2019. lidR: Airborne Lidar Data Manipulation and Visualization for Forestry. R package version 2.1.4. <http://CRAN.R-project.org/package=lidR>.
- Ryan, K. C., and T. S. Opperman. 2013. "LANDFIRE – A National Vegetation/Fuels Data Base for Use in Fuels Treatment, Restoration, and Suppression Planning." *Forest Ecology and Management* 294: 208–16.
- Saberi, S. J. 2019. "Quantifying Burn Severity in Forests of the Interior Pacific Northwest: From Field Measurements to Satellite Spectral Indices." MS thesis, University of Washington.
- Schauberger, P., and A. Walker. 2019. openxlsx: Read, Write and Edit xlsx Files. R package version 4.1.3. <https://CRAN.R-project.org/package=openxlsx>.
- Schoennagel, T., T. T. Veblen, and W. H. Romme. 2004. "The Interaction of Fire, Fuels, and Climate across Rocky Mountain Forests." *Bioscience* 54: 661–76.
- Scott, J. H., and E. D. Reinhardt. 2001. *Assessing Crown Fire Potential by Linking Models of Surface and Crown Fire Behavior*. Fort Collins, CO: USDA Forest Service, Rocky Mountain Research Station, Research Paper RMRS-RP-29.
- Sibold, J. S., K. Krasnow, and D. C. Abendroth. 2014. *Fire History of Grand Teton National Park and Surrounding Areas: Did an Historical Map from 1898 Capture the Distribution of Late 19th Century Fire?* Jackson, WY: Teton Research Institute of the Teton Science Schools.
- Spence, M. D. 1999. *Dispossessing the Wilderness: Indian Removal and the Making of the National Parks*. New York, NY: Oxford University Press.
- Spiess, A.-N. 2018. qpcR: Modelling and Analysis of Real-Time PCR Data. R package version 1.4-1. <https://CRAN.R-project.org/package=qpcR>.
- Stephens, S. L., J. K. Agee, P. Z. Fulé, M. P. North, W. H. Romme, T. W. Swetnam, and M. G. Turner. 2013. "Managing Forests and Fire in Changing Climates." *Science* 342: 41–2.

- Stevens-Rumann, C. S., S. J. Prichard, E. K. Strand, and P. Morgan. 2016. "Prior Wildfires Influence Burn Severity of Subsequent Large Fires." *Canadian Journal of Forest Research* 46: 1375–85.
- Stratton, R. D. 2009. *Guidebook on LANDFIRE Fuels Data Acquisition, Critique, Modification, Maintenance, and Model Calibration*. Fort Collins, CO: USDA Forest Service, Rocky Mountain Research Station, General Technical Report RMRS-GTR-220.
- Szpakowski, D. M., and J. L. R. Jensen. 2019. "A Review of the Applications of Remote Sensing in Fire Ecology." *Remote Sensing* 11: 2638.
- Szpakowski, D. M., J. L. R. Jensen, D. R. Butler, and T. E. Chow. 2021. "A Study of the Relationship between Fire Hazard and Burn Severity in Grand Teton National Park, USA." *International Journal of Applied Earth Observation and Geoinformation* 98: 102305.
- Tanhuanpää, T., V. Kankare, M. Väistö, N. Saarinen, and M. Holopainen. 2015. "Monitoring Downed Coarse Woody Debris through Appearance of Canopy Gaps in Urban Boreal Forests with Bitemporal ALS Data." *Urban Forestry and Urban Greening* 14: 835–43.
- Tennekes, M. 2018. "Tmap: Thematic Maps in R." *Journal of Statistical Software* 84: 1–39.
- Tinker, D. B., and D. H. Knight. 2000. "Coarse Woody Debris Following Fire and Logging in Wyoming Lodgepole Pine Forests." *Ecosystems* 3: 472–83.
- Turner, M. G., K. H. Braziunas, W. D. Hansen, and B. J. Harvey. 2019. "Short-Interval Severe Fire Erodes the Resilience of Subalpine Lodgepole Pine Forests." *Proceedings of the National Academy of Sciences* 116: 11319–28.
- Turner, M. G., W. W. Hargrove, R. H. Gardner, and W. H. Romme. 1994. "Effects of Fire on Landscape Heterogeneity in Yellowstone National Park, Wyoming." *Journal of Vegetation Science* 5: 731–42.
- Turner, M. G., and W. H. Romme. 1994. "Landscape Dynamics in Crown Fires Ecosystems." *Landscape Ecology* 9: 59–77.
- Turner, M. G., D. B. Tinker, W. H. Romme, D. M. Kashian, and C. M. Litton. 2004. "Landscape Patterns of Sapling Density, Leaf Area, and Aboveground Net Primary Production in Post-fire Lodgepole Pine Forests, Yellowstone National Park (USA)." *Ecosystems* 7: 751–75.
- USDA Forest Service. 2019. Insect and Disease Detection Survey (IDS) Data for Region 4. <https://www.fs.fed.us/foresthealth/applied-sciences/mapping-reporting/detection-surveys.shtml>.
- van Aardt, J. A. N., M. Arthur, G. Sovkopal, and T. L. Swetnam. 2011. "Lidar-Based Estimation of Forest Floor Fuel Loads Using a Novel Distributional Approach." In *SilviLaser 2011 (Conf)* 1–8. Hobart, TAS, Australia: University of Tasmania.
- Van Wagner, C. E. 1977. "Conditions for the Start and Spread of Crown Fire." *Canadian Journal of Forest Research* 7: 23–34.
- Van Wagner, C. E. 1989. "Prediction of Crown Fire in Conifer Stands." In *10th Conference on Fire and Forest Meteorology*, edited by D. C. MacIver, H. Auld, and R. Whitewood, 207–12. Ottawa, ON: Forestry Canada and Environment Canada.
- Wei, T., and V. Simko. 2017. corrplot: Visualization of a Correlation Matrix. R package version 0.84. <https://github.com/taiyun/corrplot>.
- Weise, D. R., and C. S. Wright. 2014. "Wildland Fire Emissions, Carbon and Climate: Characterizing Wildland Fuels." *Forest Ecology and Management* 317: 26–40.
- Westerling, A. L. 2016. "Increasing Western US Forest Wildfire Activity: Sensitivity to Changes in the Timing of Spring." *Philosophical Transactions of the Royal Society B: Biological Sciences* 371: 20150178.
- Western Regional Climate Center (WRCC). 2020a. Cooperative Climatological Data Summaries: NOAA Cooperative Stations – Temperature and Precipitation. Moose, Wyoming (Station 486428). <https://wrcc.dri.edu/cgi-bin/cliMAIN.pl?wy6428>.
- Western Regional Climate Center (WRCC). 2020b. RAWS USA Climate Archive: Grand Teton Wyoming Remote Automated Weather Station. <https://raws.dri.edu/cgi-bin/rawMAIN.pl?wyWGRA>.
- White, J. C., M. A. Wulder, A. Varhola, M. Väistö, N. C. Coops, B. D. Cook, D. Pitt, and M. Woods. 2013. *A Best Practices Guide for Generating Forest Inventory Attributes from Airborne Laser Scanning Data Using an Area-Based Approach (Version 2.0)*. Victoria, BC: Canadian Forest Service, Canadian Wood Fibre Centre, Information Report FI-X-010.
- Whitlock, C., P. E. Higuera, D. B. McWethy, and C. E. Briles. 2010. "Paleoecological Perspectives on Fire Ecology: Revisiting the Fire-Regime Concept." *The Open Ecology Journal* 3: 6–23.
- Whitlock, C., J. Marlon, C. Briles, A. Brunelle, C. Long, and P. Bartlein. 2008. "Long-Term Relations among Fire, Fuel, and Climate in the North-Western US Based on Lake-Sediment Studies." *International Journal of Wildland Fire* 17: 72–83.
- Wickham, H., M. Averick, J. Bryan, W. Chang, L. McGowan, R. François, G. Grolemund, et al. 2019. "Welcome to the Tidyverse." *Journal of Open Source Software* 4: 1686.
- Wildland Fire Executive Council (WFEC). 2014. *The National Strategy: The Final Phase in the Development of the National Cohesive Wildland Fire Management Strategy*. Washington, DC: Wildland Fire Executive Council.
- Woolpert. 2015. *Grand Teton and National Elk Refuge Lidar Processing*. Rolla, MO: USGS.
- Yellowstone National Park (YNP). 2017. *Yellowstone Resources and Issues Handbook: 2017*. Park County, WY: Yellowstone National Park.
- Zhao, F., R. A. Sweitzer, Q. Guo, and M. Kelly. 2012. "Characterizing Habitats Associated with Fisher Den Structures in the Southern Sierra Nevada, California Using Discrete Return Lidar." *Forest Ecology and Management* 280: 112–9.
- Zvoleff, A. 2020. glcm: Calculate Textures from Grey-Level Co-Occurrence Matrices (GLCMs). R package version 1.6.5. <https://CRAN.R-project.org/package=glcm>.

SUPPORTING INFORMATION

Additional supporting information may be found in the online version of the article at the publisher's website.

How to cite this article: Braziunas, Kristin H., Diane C. Abendroth, and Monica G. Turner. 2022. "Young Forests and Fire: Using Lidar-Imagery Fusion to Explore Fuels and Burn Severity in a Subalpine Forest Reburn." *Ecosphere* 13(5): e4096. <https://doi.org/10.1002/ecs2.4096>

**Young forests and fire: Using lidar-imagery fusion to
explore fuels and burn severity in a subalpine forest reburn**

Kristin H. Braziunas, Diane C. Abendroth, and Monica G. Turner

Journal: Ecosphere

Appendix S1: Supplemental tables and figures

Table S1. Regression model predictor variables from lidar point clouds and NAIP imagery.

DN: digital number, NIR: near infrared, NDVI: Normalized Difference Vegetation Index.

| Predictor variable | Description |
|-------------------------------|--|
| <i>Lidar height variables</i> | |
| zmean | Mean height of point cloud (m) |
| zmin | Minimum height of point cloud (m) |
| zp10 | 10 th percentile point cloud height (m) |
| zp25 | 25 th percentile point cloud height (m) |
| zp50 | 50 th percentile point cloud height (m) |
| zp75 | 75 th percentile point cloud height (m) |
| zp90 | 90 th percentile point cloud height (m) |
| zp99 | 99 th percentile point cloud height (m) |
| zfcc | Fractional canopy cover, the number of first returns in the canopy layer (2-60 m) divided by the number of total first returns x 100 (%) |
| zfsc | Fractional shrub cover, the number of first returns in the surface layer (0-2 m) divided by the number of total first returns x 100 (%) |
| <i>NAIP imagery variables</i> | |
| Rmean | Red band – mean DN value |
| Rmin | Red band – minimum DN value |
| Rmax | Red band – maximum DN value |
| Rsd | Red band – DN standard deviation |
| Rcv | Red band – DN coefficient of variation |
| Rhom | Red band – homogeneity texture |
| Gmean | Green band – mean DN value |
| Gmin | Green band – minimum DN value |
| Gmax | Green band – maximum DN value |
| Gsd | Green band – DN standard deviation |
| Gcv | Green band – DN coefficient of variation |
| Ghom | Green band – homogeneity texture |
| Bmean | Blue band – mean DN value |
| Bmin | Blue band – minimum DN value |
| Bmax | Blue band – maximum DN value |
| Bsd | Blue band – DN standard deviation |
| Bcv | Blue band – DN coefficient of variation |
| Bhom | Blue band – homogeneity texture |
| NIRmean | NIR band – mean DN value |
| NIRmin | NIR band – minimum DN value |
| NIRmax | NIR band – maximum DN value |
| NIRsd | NIR band – DN standard deviation |
| NIRcv | NIR band – DN coefficient of variation |
| NIRhom | NIR band – homogeneity texture |
| NDVI _{mean} | Pseudo-NDVI – mean value |
| NDVI _{min} | Pseudo-NDVI – minimum value |
| NDVI _{max} | Pseudo-NDVI – maximum value |
| NDVI _{sd} | Pseudo-NDVI – standard deviation |
| NDVI _{cv} | Pseudo-NDVI – coefficient of variation |
| NDVI _{hom} | Pseudo-NDVI – homogeneity texture |

Table S2. Best model equations for predicting vegetation structure and fuels. Predictor variables are listed in order of predictive power based on partial R². Refer to Tables 1 and Appendix S1: Table S1 for descriptions of predictor and metric variables. Note that the sagebrush cover model was fit to the proportion of sagebrush cover relative to total sapling/shrub cover.

| Structure or fuels metric | Vegetation type(s) included in model | Metric transformation | Model formula (includes back-transformation) |
|--|--|-----------------------|--|
| <i>Forest structure</i> | | | |
| Tree density (stems ha ⁻¹) | Conifer, Deciduous (<i>n</i> = 28) | Natural log | $\exp(8.9248 + 0.0423 \text{ NIRmin} - 7.4676 \text{ NIRhom} + 0.0318 \text{ zfsc} - 0.0337 \text{ Bmean} + 0.0141 \text{ Rmax})$ |
| Tree basal area (m ² ha ⁻¹) | Conifer, Deciduous (<i>n</i> = 28) | Square root | $(1.6689 + 8.0154 \text{ NDVImean} + 0.0328 \text{ zfcc} - 0.0159 \text{ zcv})^2$ |
| <i>Canopy fuel layer</i> | | | |
| Canopy cover (%) | Conifer, Deciduous (<i>n</i> = 28) | — | $-32.1325 + 0.6202 \text{ zfcc} + 133.6369 \text{ NDVImax} + 0.5714 \text{ NIRmin} - 1.4850 \text{ zp99} - 0.2486 \text{ Bmax}$ |
| Canopy height (m) | Conifer, Deciduous (<i>n</i> = 28) | — | $-14.7641 + 0.9756 \text{ zmean} + 44.1452 \text{ NDVImean} + 0.2180 \text{ NIRcv} + 34.4053 \text{ NDVIhom} - 23.2282 \text{ Bhom}$ |
| Canopy fuel load (kg m ⁻²) | Conifer (<i>n</i> = 23) | Square root | $(2.3476 - 0.0183 \text{ Rmean} - 0.0222 \text{ zp99} - 0.0045 \text{ zcv} + 3.3351 \text{ NDVIstd})^2$ |
| Canopy bulk density (kg m ⁻³) | Conifer (<i>n</i> = 23) | Cube root | $(0.5018 - 0.0111 \text{ zp99} - 0.0041 \text{ Rmean} + 3.2130 \text{ NDVIstd} + 0.5273 \text{ NDVImin})^3$ |
| Canopy base height (m) | Conifer (<i>n</i> = 23) | Square root | $(-0.5830 - 13.6975 \text{ NDVIstd} - 3.4047 \text{ NDVImin} + 4.2769 \text{ NDVIhom} + 2.7637 \text{ NDVImax} - 1.8579 \text{ Bhom})^2$ |
| <i>Surface fuel layer</i> | | | |
| Coarse woody debris cover (%) | Conifer (<i>n</i> = 23) | — | $-26.9737 + 75.2377 \text{ NDVImean} + 0.8523 \text{ Gmin} + 0.2412 \text{ zcv} + 139.8889 \text{ NDVIstd} - 0.2733 \text{ NIRmax}$ |
| Coarse woody debris biomass (Mg ha ⁻¹) | Conifer (<i>n</i> = 23) | Natural log | $\exp(-9.9199 + 0.1534 \text{ Gmin} + 8.6478 \text{ NDVImean} + 0.0339 \text{ zcv} + 0.1109 \text{ Bcv} + 0.0549 \text{ zp99})$ |
| Sapling/shrub cover (%) | Conifer (<i>n</i> = 23) | — | $142.7305 - 0.6420 \text{ Rmax} - 2.0016 \text{ zp50} + 0.5731 \text{ NIRcv} - 66.7153 \text{ NDVImin} - 81.3023 \text{ NDVIhom}$ |
| Sapling/shrub height (m) | Conifer (<i>n</i> = 23) | — | $3.3391 - 0.0256 \text{ NIRmean} - 0.0312 \text{ Rev} + 0.0165 \text{ zfsc} + 3.2889 \text{ NDVImin} + 0.0837 \text{ Bsd}$ |
| Sapling/shrub cover (%) | Shrubland (<i>n</i> = 15) | — | $33.2757 + 367.5209 \text{ NDVImean} - 151.2069 \text{ zp50} - 318.7225 \text{ NDVImin}$ |
| Sapling/shrub height (m) | Shrubland (<i>n</i> = 15) | — | $-0.1734 + 0.0085 \text{ zfsc} + 1.2663 \text{ NDVImean} + 0.5527 \text{ Bhom}$ |
| Sapling/shrub percent dead | Shrubland (<i>n</i> = 15) | Cube root | $(7.5146 - 0.0373 \text{ Gmax} + 0.1262 \text{ NIRcv} - 1.4452 \text{ NDVImax})^3$ |
| Sagebrush cover (proportion) | Shrubland (<i>n</i> = 15) | — | $0.4667 - 15.6064 \text{ NDVIstd} + 1.3729 \text{ NIRhom} + 0.8867 \text{ zp50}$ |

Table S3. Percent of fuel and structure metrics that were reclassified to minimum or maximum values.

| Structure or fuels metric | Cells below min (%) | Cells above max (%) | Total outside bounds (%) |
|-----------------------------|---------------------|---------------------|--------------------------|
| <i>Forest</i> | | | |
| Tree density | 0 | 0.03 | 0.03 |
| Tree basal area | 0 | 0 | 0 |
| Canopy cover | 4.3 | 0.02 | 4.3 |
| Canopy height | 1.2 | 0 | 1.2 |
| Canopy fuel load | 0 | 0.06 | 0.06 |
| Canopy bulk density | 2.0 | 0.5 | 2.4 |
| Canopy base height | 0 | 1.8 | 1.8 |
| Coarse woody debris cover | 14.8 | 0.1 | 14.9 |
| Coarse woody debris biomass | 0 | 6.2 | 6.2 |
| Sapling/shrub cover | 21.9 | 1.3 | 23.2 |
| Sapling/shrub height | 3.6 | 5.1 | 8.7 |
| All forest metrics | 4.3 | 1.5 | 5.7 |
| <i>Shrubland</i> | | | |
| Sapling/shrub cover | 5.5 | 2.5 | 7.9 |
| Sapling/shrub height | 0.009 | 0 | 0.009 |
| Sapling/shrub percent dead | 0 | 3.2 | 3.2 |
| Proportion sagebrush | 7.6 | 37.2 | 44.8 |
| All shrubland metrics | 3.3 | 10.7 | 14.0 |
| <i>All metrics</i> | 4.1 | 3.9 | 7.9 |

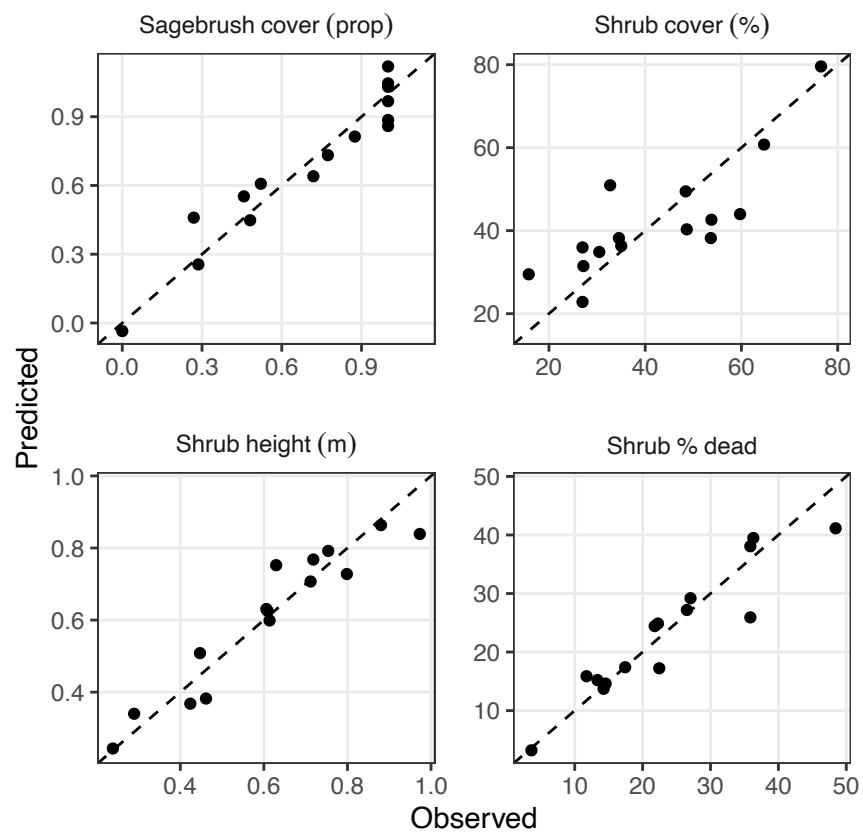


Figure S1. Predicted versus observed (field data) values for final shrubland regression models ($n = 15$). Dashed lines are 1:1 lines.

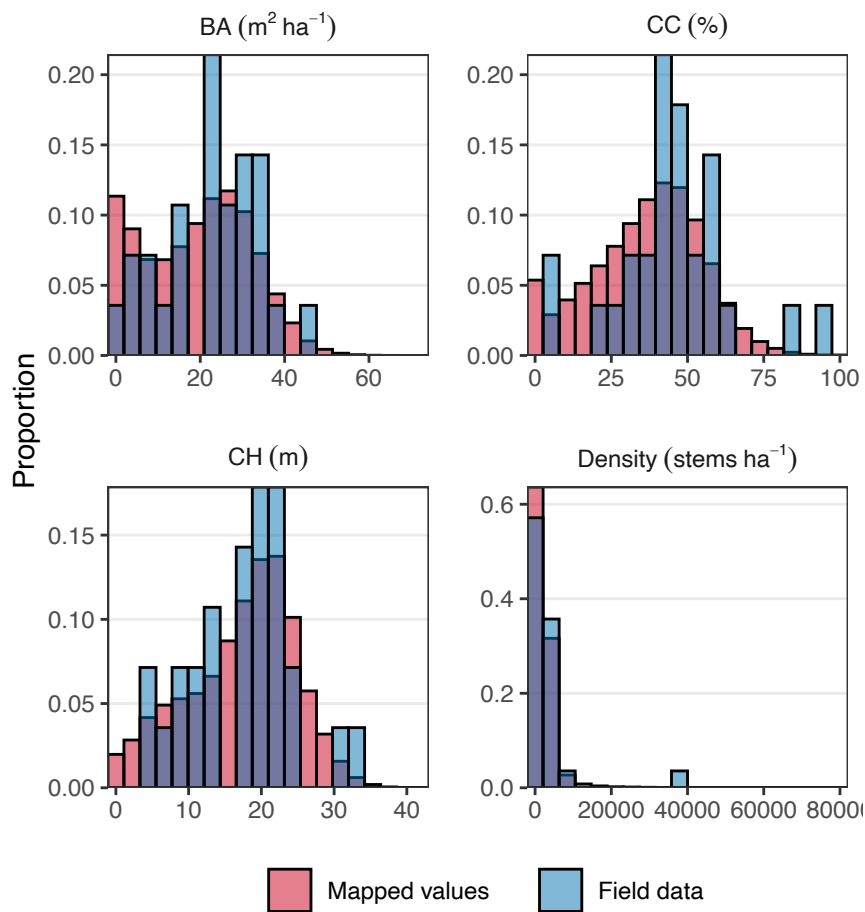


Figure S2. Histograms showing distribution of mapped values ($n = 534,052$; blue) versus field data observations ($n = 28$, red) for combined conifer and deciduous forest. Includes canopy fuel metrics and forest structure. Overlapping areas are in purple. Refer to Table 1 for abbreviations.

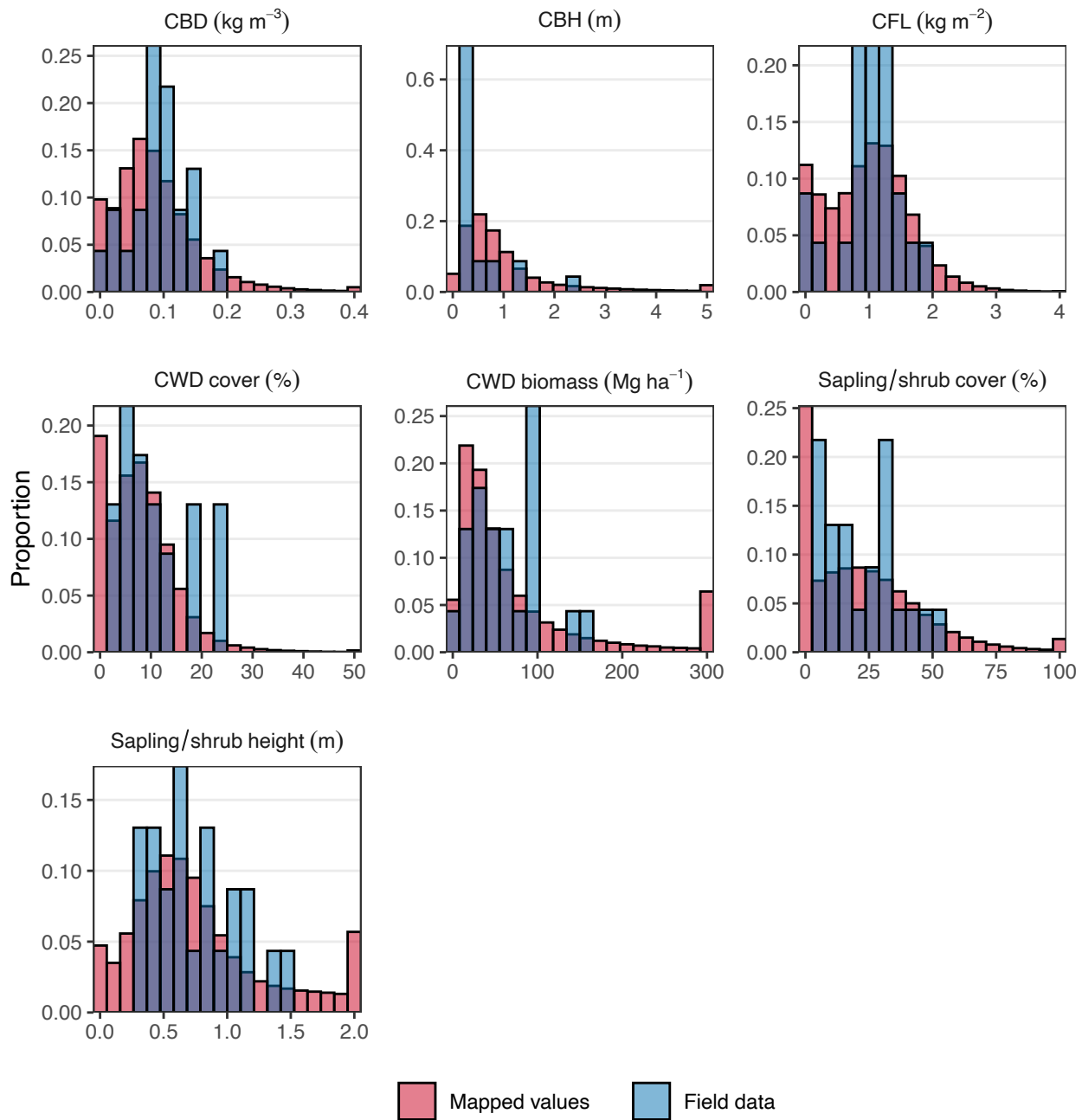


Figure S3. Histograms showing distribution of mapped values ($n = 505,250$; blue) versus field data observations ($n = 23$, red) for conifer forest. Includes canopy and surface fuel metrics. Overlapping areas are in purple. Refer to Table 1 for abbreviations.

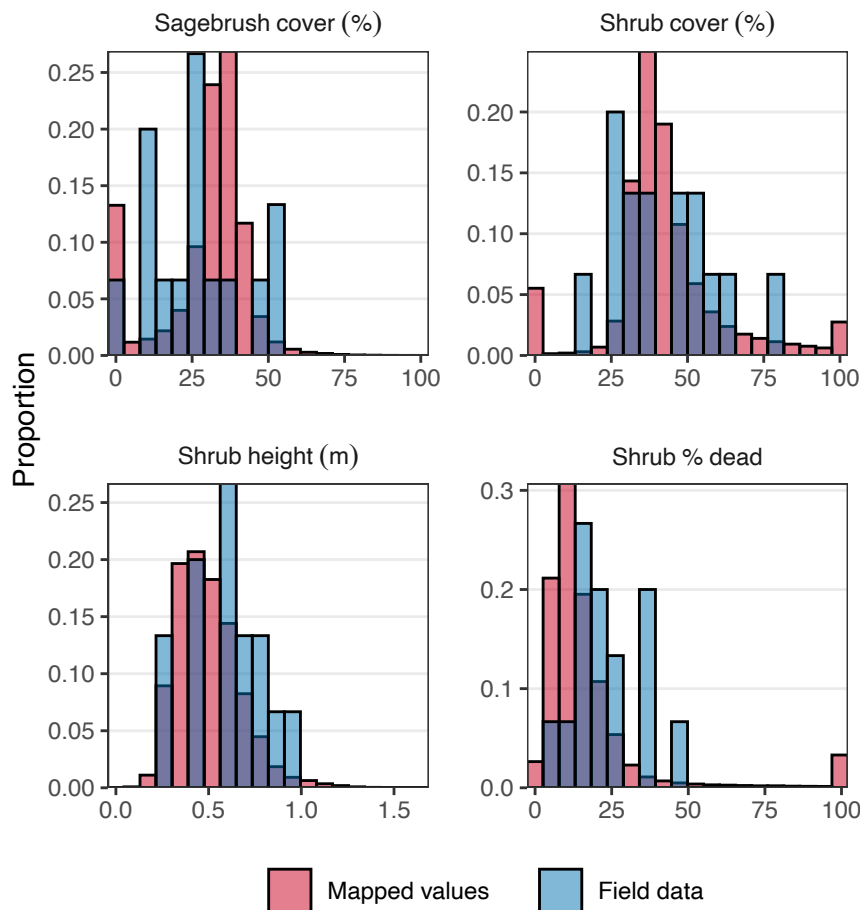


Figure S4. Histograms showing distribution of mapped values ($n = 312,047$; blue) versus field data observations ($n = 15$, red) for shrubland. Includes surface fuel metrics and other shrubland variables. Overlapping areas are in purple. Refer to Table 1 for abbreviations.

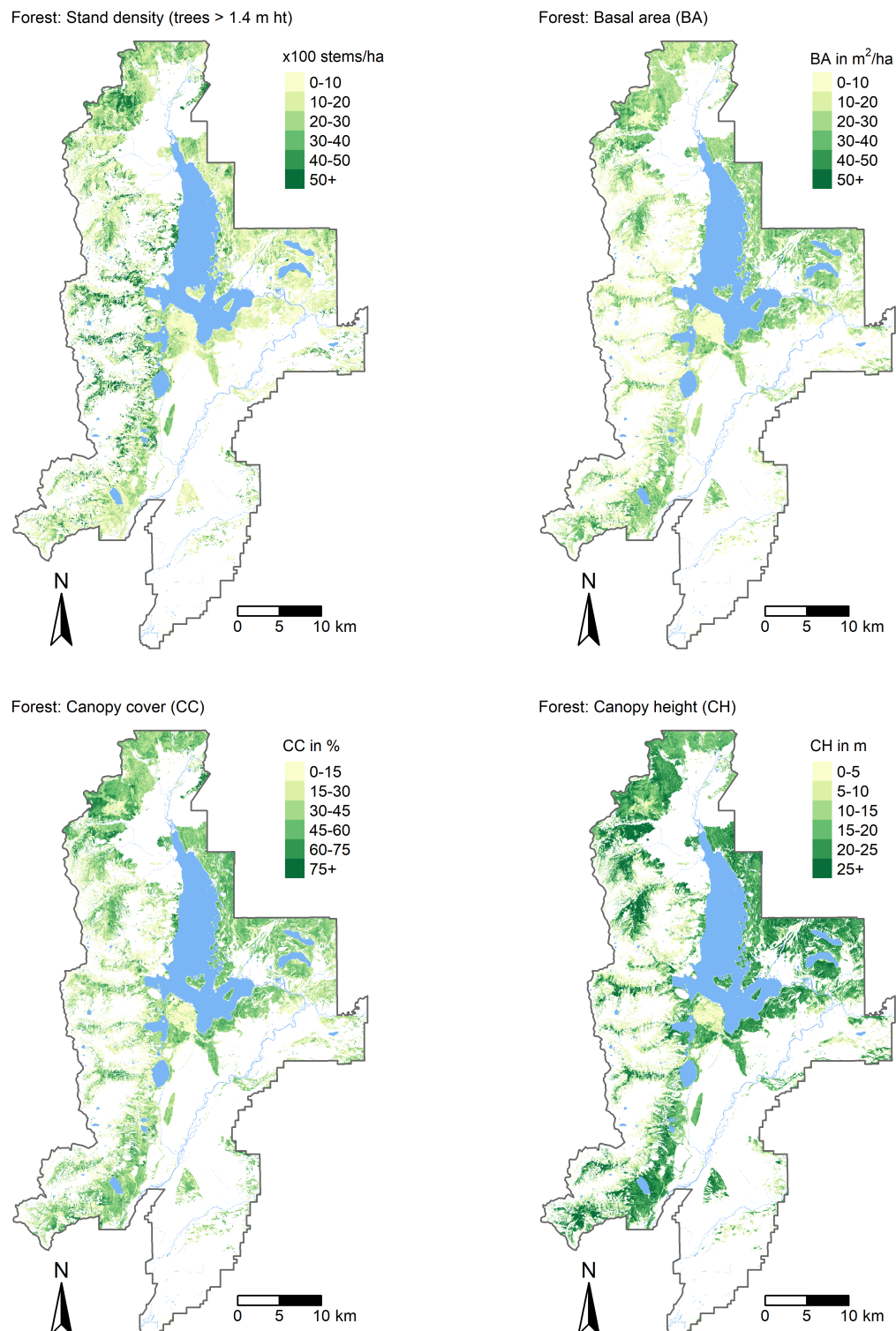


Figure S5. Forest structure and fuels maps for combined conifer and deciduous forest at 30-m resolution. Water is shown in blue.

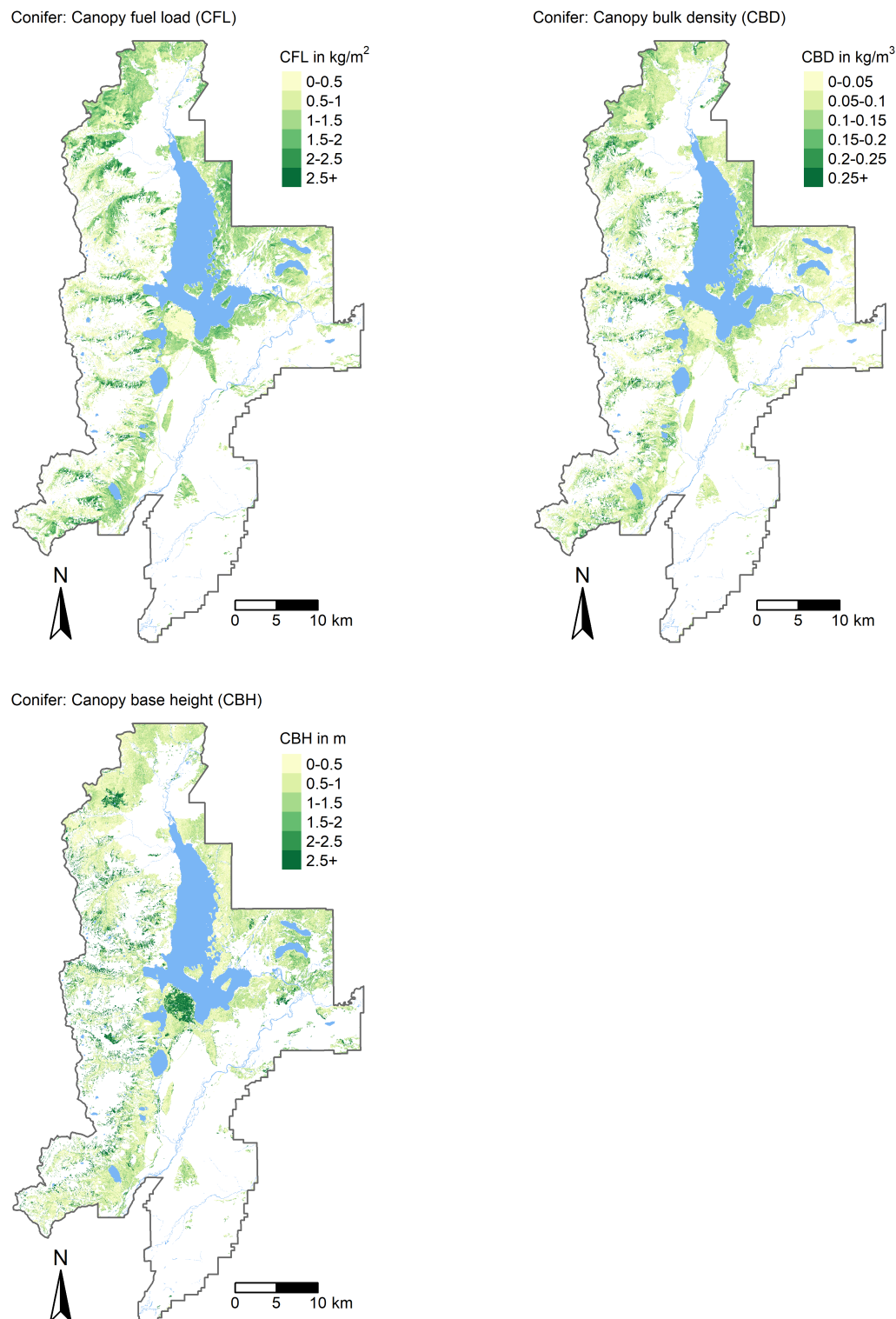


Figure S6. Canopy fuels maps for conifer forest at 30-m resolution. Water is shown in blue.

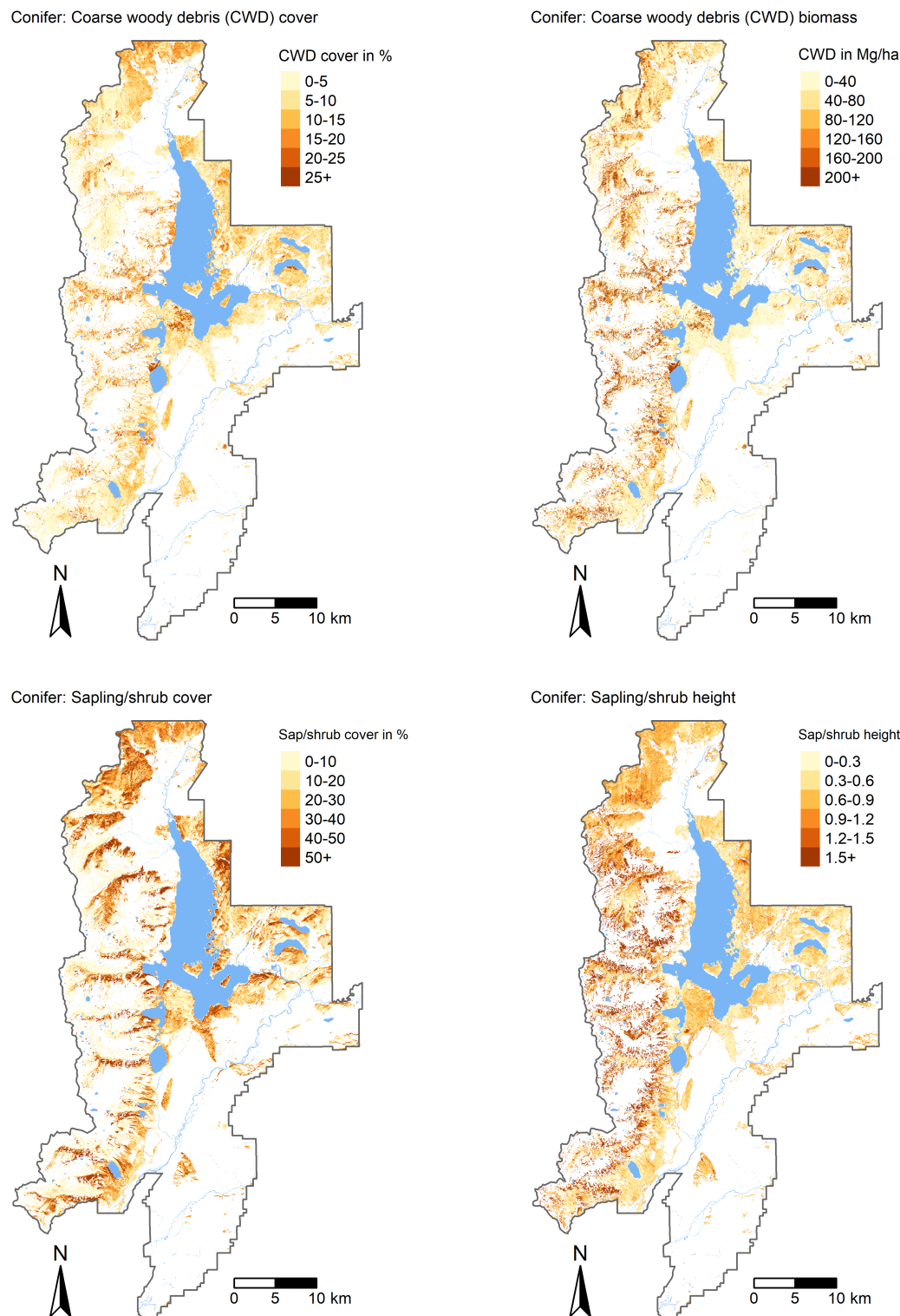


Figure S7. Surface fuels maps for conifer forest at 30-m resolution. Water is shown in blue.

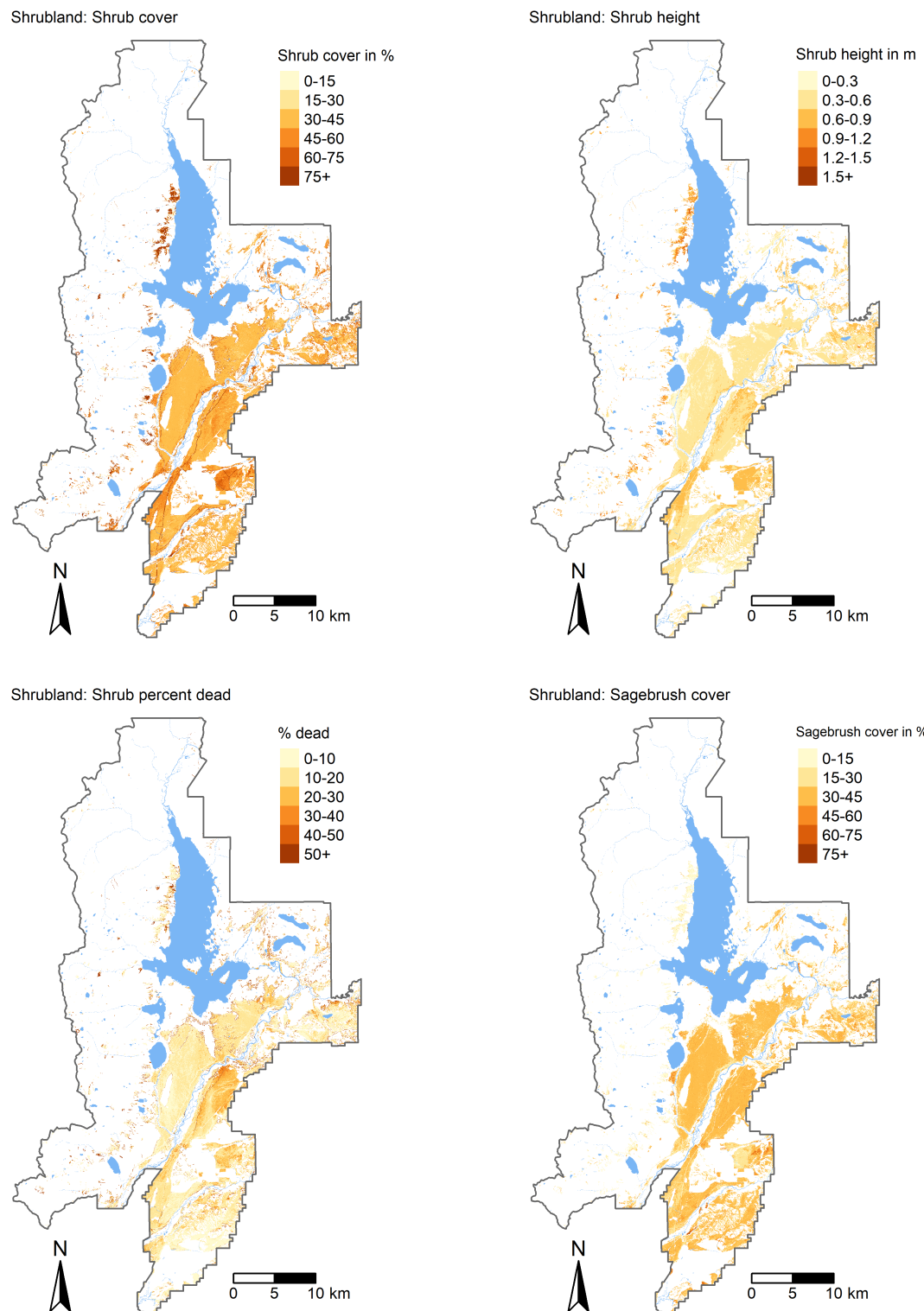


Figure S8. Vegetation and fuels maps for shrubland at 30-m resolution. Water is shown in blue.

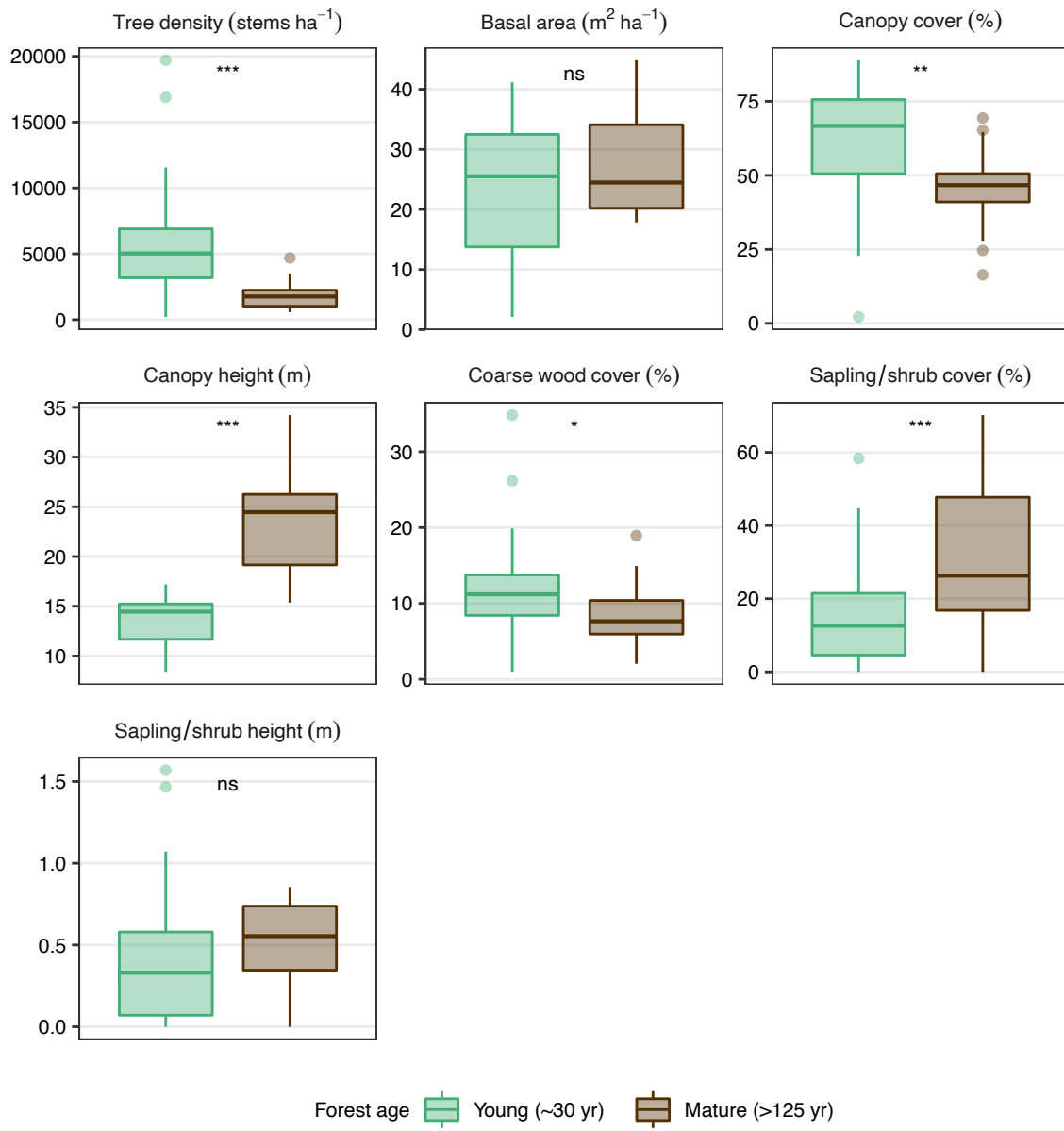


Figure S9. Forest structure and fuels in young (~30-year-old, green) compared to mature (>125-year-old, brown) forests that burned during the 2016 Berry Fire. Bold lines show the median value, boxes show the interquartile range (IQR), and whiskers extend 1.5 x IQR or to the most extreme data point. Results of Wilcoxon rank-sum tests indicate whether differences between distributions are not statistically significant (ns) or statistically significant at $p < 0.05$ (*), $p < 0.01$ (**), or $p < 0.001$ (***)�.

**Young forests and fire: Using lidar-imagery fusion to
explore fuels and burn severity in a subalpine forest reburn**

Kristin H. Braziunas, Diane C. Abendroth, and Monica G. Turner

Journal: Ecosphere

Appendix S2: Comparison of lidar-imagery fusion and LANDFIRE fuels maps with field data

We compared final lidar-imagery fusion fuels maps, as well as LANDFIRE (LANDFIRE 2016) fuels maps, with our field data for the four canopy fuels metrics mapped by LANDFIRE: canopy cover, canopy height, canopy bulk density, and canopy base height ($n = 28$ observations for canopy cover and height; $n = 23$ for canopy bulk density and base height; Figure S1). We used field data plot centroids to extract the corresponding raster values and assessed goodness-of-fit with a linear regression.

Lidar-imagery fusion fuels maps better predicted field-measured canopy fuels than LANDFIRE. Goodness-of-fit was highest for canopy height ($R^2 = 0.77$ and 0.38 for lidar-imagery fusion and LANDFIRE, respectively), followed by canopy cover ($R^2 = 0.46$ and 0.14), canopy base height ($R^2 = 0.42$ and 0.19), and canopy bulk density ($R^2 = 0.19$ and 0.04). LANDFIRE had a negative relationship with canopy base height, but this was strongly driven by only two plots (Figure S1). Because we used the same field data to build the lidar-imagery fusion models predicting fuels, these plots should not be considered an independent validation of our final fuels maps. Low goodness-of-fit values for some metrics could be due in part to the

mismatch between plot and raster cell footprint location and size (field plots were 530 m² and fuels map pixels are 900 m²). Fuels metrics that exhibit greater variability at fine scales may be more sensitive to these differences, and lidar and imagery predictor values may also be sensitive to plot size.

Literature cited

LANDFIRE. 2016. LANDFIRE 2.0.0 Canopy Cover, Canopy Height, Canopy Bulk Density, and Canopy Base Height layers. US Department of the Interior, US Geological Survey.
<https://landfire.cr.usgs.gov/viewer/> (Accessed April 26, 2019).

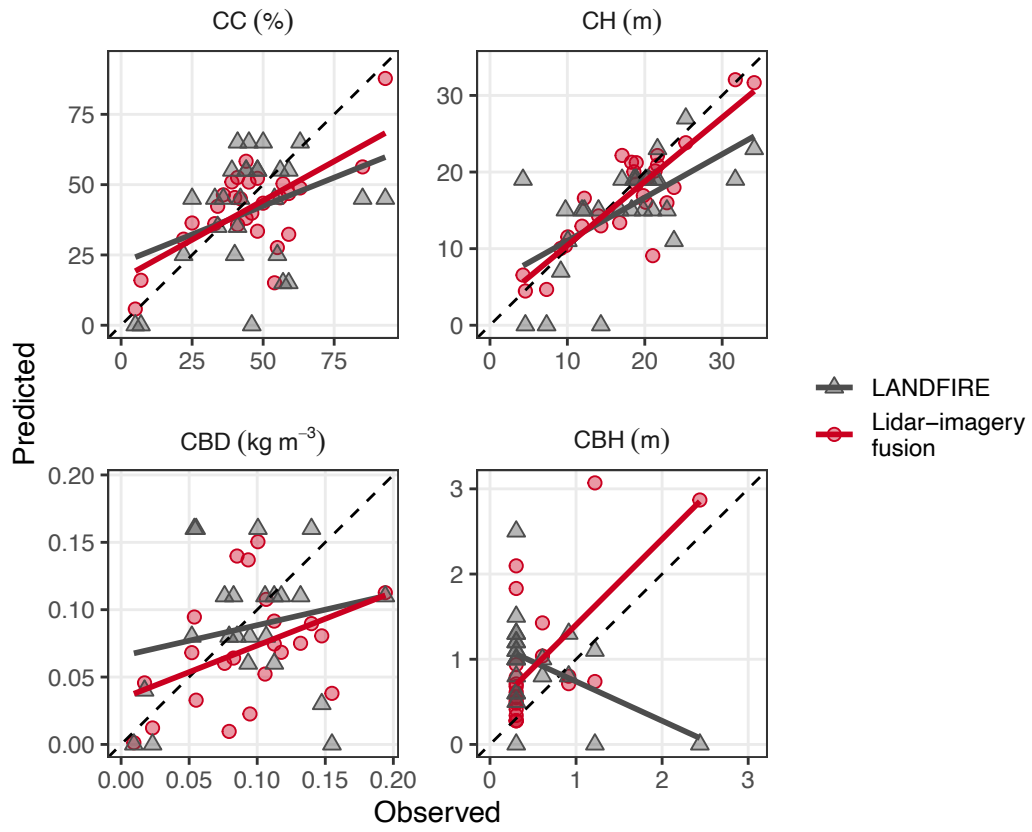


Figure S1. Comparison of lidar-imagery fusion and LANDFIRE canopy fuels maps with field data ($n = 28$ for canopy cover and height; $n = 23$ for canopy bulk density and base height). Points are predicted versus observed values for lidar-imagery fusion (red circles) and LANDFIRE (gray triangles), dashed lines are 1:1 lines, and solid lines are linear fits to predicted versus observed values. CC: canopy cover, CH: canopy height, CBD: canopy bulk density, CBH: canopy base height.